Journal of Renewable Materials

Tech Science Press

https://doi.org/10.32604/jrm.2026.02025-0190

REVIEW

Advances in Cellulose-Based Materials: A Comprehensive Review of Functionalization and Processing for Water Remediation

Wafaa Abou-Elseoud and Mohammad Hassan*

Cellulose and Paper Department & Center of Excellence for Advanced Sciences, Advanced Materials and Nanotechnology Group, National Research Centre, Giza, Egypt

*Corresponding Author: Mohammad Hassan. Email: ml.hassan@nrc.sci.eg or mlhassan2012@gmail.com

Received: 09 October 2025; Accepted: 06 March 2026; Published: 29 June 2026

ABSTRACT: Cellulose-based materials have emerged as promising biomaterials for advanced water remediation technologies due to their bioavailability, non-toxicity, biocompatibility, hydrophilicity, and ease of chemical modification. Cellulose can be prepared in multiple forms, including nanomaterials such as cellulose nanofibrils (CNFs), cellulose nanocrystals (CNCs), and electrospun nanofibers. The abundant surface functional groups, such as hydroxyl and carboxyl groups, enable chemical tailoring, grafting, and composite formation with organic and inorganic additives, including metal–organic frameworks (MOFs), carbon-based materials, and metal oxide nanoparticles. These modifications enhance pollutant removal through adsorption, catalysis, and antimicrobial activity, enabling the treatment of heavy metals, dyes, pharmaceuticals, pesticides, oils, and microbial contaminants. Cellulosic materials can be engineered into diverse structures such as membranes, aerogels, filters, papers, and foams. This review discusses two major approaches for water remediation: cellulose-based systems—including smart composites, MOF-integrated materials, photocatalytic membranes, and chemically modified derivatives—and nanocellulose-based systems utilizing CNF, CNC, electrospun fibers, and bacterial cellulose for efficient pollutant removal. Future work should focus on developing cellulose-based materials containing both anionic and cationic groups, as well as advancing cellulose–MOF composites with higher surface area and lower density to improve adsorption efficiency.

KEYWORDS: Cellulose; stimuli-responsive; metal organic frameworks; nanocellulose; composites; water remediation

1 Introduction

Water is indispensable for all forms of life, yet the scarcity of safe freshwater has made pollution one of the most pressing global environmental challenges. Industrialization and population growth have contributed significantly to the deterioration of water quality, generating large volumes of contaminated wastewater. The United Nations' Global Water Development Report estimates that nearly two million tons of waste are produced daily from industrial activities, including chemical discharges, sewage, and mining by-products, while agricultural practices add further stress through the release of fertilizers and pesticides into water bodies [1]. Consequently, polluted water often contains hazardous organic and inorganic contaminants such as heavy metals, dyes, phenols, pesticides, and insecticides [2]. Prolonged exposure to these pollutants has been linked to severe health outcomes, including respiratory and cardiovascular diseases, kidney failure, and reduced life expectancy [3]. To address these concerns, several remediation techniques have been employed before wastewater discharge, including reverse osmosis [4], photodegradation [5], coagulation [6],

filtration [7], and adsorption [8] (Table 1). Among these, adsorption stands out as an efficient and cost-effective strategy adaptable to diverse contaminants, though its effectiveness is highly dependent on the choice of adsorbent materials.

Table 1: Comparison of wastewater treatment techniques.

Technique	Advantages	Limitations	Cost	Efficiency	Environmental Impact	Operational Complexity
Reverse Osmosis	Removes salts, heavy metals, microorganisms, and most organic contaminants; highly effective	Membrane fouling; requires high pressure; produces brine waste	High (installation + energy)	Very high	Produces concentrated waste streams requiring disposal	High due to energy demand and maintenance
Photodegradation (e.g., photocatalysis)	Can fully degrade pollutants into harmless products; no chemical additives	Requires UV/solar activation; limited efficiency in turbid wastewater; catalyst recovery needed	Moderate to high	High for certain organics	Generally eco-friendly but may involve nanoparticle residues	Moderate; depends on light source and reactor design
Coagulation/ Flocculation	Fast and effective for suspended solids, dyes, and some organics; simple equipment	Generates large sludge volume; continuous chemical input	Moderate	Moderate to high	Potential chemical residues and sludge disposal issues	Low to moderate
Filtration (e.g., sand, activated carbon filters)	Simple, low energy; effective for particulates and some dissolved substances	Media saturation requires regeneration or replacement; limited removal of dissolved pollutants alone	Low to moderate	Moderate	Low environmental impact if natural media is used	Low
Adsorption	Effective for a wide range of pollutants; adsorbents can be low-cost and regenerated; simple to operate	Performance depends on adsorbent type and regeneration conditions	Low to moderate	High	Minimal secondary waste, especially with bio-based adsorbents	Low; requires no advanced equipment

In recent years, polysaccharide-based composites have emerged as promising sustainable adsorbents for water remediation [9]. Polysaccharides are natural, biodegradable, and abundantly available biopolymers with a high density of functional groups, making them easily modifiable for the design of tailor-made adsorbents [10]. Their eco-friendly nature and versatility have positioned them as viable alternatives to conventional synthetic adsorbents. Previous research has demonstrated the successful application of polysaccharide composites such as cyclodextrin [11], chitosan [12], and cellulose [13] in removing a wide range of pollutants from wastewater. However, despite these advances, further studies are required to optimize their performance, improve adsorption efficiency, and assess their practicality under real-world environmental

conditions. These efforts are critical for advancing polysaccharide-based composites as sustainable materials capable of contributing to long-term water quality protection and environmental health.

Cellulose as a Renewable Biopolymer for Water Remediation

Cellulose is a long, straight-chain polysaccharide distinguished by its tasteless, odorless, and hydrophilic nature [14]. Although generally insoluble in water and many inorganic solvents, cellulose is biodegradable, renewable, and environmentally benign, which makes it particularly attractive for sustainable applications. Structurally, cellulose consists of repeating units of D-anhydroglucopyranose connected by β-1,4-glycosidic bonds, with varying degrees of polymerization leading to the formation of organized microfibrils. Each repeating unit contains three hydroxyl groups, which provide abundant reactive sites for chemical modification and enable the preparation of a wide range of cellulose derivatives through well-established alcohol chemistry.

In recent years, cellulose and its derivatives have been widely investigated for wastewater remediation due to their availability, low cost, and tunable surface chemistry. Modified cellulose materials including hydrogels, nanocellulose, and cellulose-based composites have demonstrated remarkable adsorption capabilities toward heavy metals, dyes, and organic pollutants [15–17]. For instance, cationic cellulose derivatives have achieved high adsorption capacities for anionic dyes in real wastewater systems, while cellulose-based nanofiltration membranes have removed over 98% of methylene blue with excellent re-usability [17]. Reinforced cellulose filter papers have also shown simultaneous removal of dyes and oil emulsions with >99% efficiency and improved stability [18]. Despite these advances, most studies have been limited to laboratory conditions, single-pollutant systems, or high-cost modification processes, which constrain large-scale application. Therefore, further research is required to optimize cellulose-based adsorbents, enhance their performance under realistic wastewater conditions, and design eco-friendly composites with practical applicability. This review focuses on recent advances in water remediation using nano-cellulosic materials. It highlights two key strategies: smart cellulose composites and cellulose-based metal–organic framework (MOF) composites. It also examines the application of various nanocellulose forms—including CNF, electrospun CNF, CNC, and bacterial cellulose—for removing different water contaminants.

2 Cellulose Nanomaterials (Nanocellulose)

In the hierarchical structure of cellulose, the crystalline regions formed by tightly packed lignocellulosic domains confer strength and rigidity, while the amorphous regions provide flexibility to the biomass [19]. Nanocelluloses can be isolated from native cellulose in both crystalline and fibrous forms, with dimensions in the nanometer range and diameters typically below 100 nm [20]. Owing to their superior mechanical, optical, and chemical properties at the nanoscale compared to bulk cellulose, nanocelluloses are considered ideal materials for advanced applications [21]. Depending on the isolation method, cellulose nanomaterials are generally categorized into four classes: electrospun cellulose nanofibers, cellulose nanofibrils (CNFs), cellulose nanocrystals (CNCs), and bacterial nanocellulose (BNC).

2.1 Electrospun Cellulose Nanofibers

Electrospinning is a promising technique for producing cellulose nanofibers with diameters ranging from 100 nm to several micrometers [22]. In this process, a high voltage overcomes surface tension, drawing the polymer jet toward a grounded collector where it solidifies into interconnected fibers. However, direct electrospinning of cellulose remains challenging due to its poor solubility and difficulty in melt processing, often requiring chemical modification or dissolution in specialized solvents.

2.2 Cellulose Nanofibrils (CNFs)

Cellulose nanofibrils consist of flexible fibrils with diameters in the nanometer range and lengths on the micrometer scale, forming a highly entangled network structure [21]. Similar to microfibrillated cellulose, CNFs contain both crystalline and amorphous domains [23]. They can be produced using several mechanical disintegration techniques, including ultrafine grinding, high-pressure homogenization, ball milling, and ultrasonication [23]. Among these, ball milling is frequently employed due to its simplicity and scalability, though it requires high energy input and can be costly [24,25]. To address these limitations, pretreatments such as acid hydrolysis, oxidation, or enzymatic treatment are often applied to weaken hydrogen bonding and disrupt amorphous regions, thereby reducing energy consumption during fibrillation [26,27].

2.3 Cellulose Nanocrystals (CNCs)

Cellulose nanocrystals (CNCs), also known as nanowhiskers, are rod-like nanoparticles typically 1–50 nm in width and a few hundred nanometers in length, depending on the source material [28]. Compared to CNFs, CNCs possess higher crystallinity, greater surface area, and superior mechanical and liquid-crystalline properties [29]. Several techniques are used for their isolation, including acid hydrolysis, subcritical water hydrolysis, and ionic liquid treatment [30]. Among these, acid hydrolysis with strong acids such as sulfuric, hydrochloric, or phosphoric acid remains the most common method due to its efficiency, though it often requires careful optimization to balance yield and stability [31,32].

2.4 Bacterial-Based Cellulose

Bacterial cellulose (BC) is a highly pure form of cellulose produced by microorganisms such as *Acetobacter xylinum* and *Gluconacetobacter xylinus* [33]. The diameter of BC fibers typically ranges from 25 to 45 nm, with variations depending on bacterial strain and incubation conditions [34]. BC exhibits a unique three-dimensional nanofibrillar network, characterized by high crystallinity, a high degree of polymerization, excellent mechanical strength, and remarkable water-holding capacity. These attributes make BC particularly attractive for biomedical, food packaging, and wastewater remediation applications [35].

3 Nanocellulose-Based Composites for Water Remediation

Nanocellulosic materials have emerged as sustainable and efficient components for water remediation due to their abundance, renewability, biodegradability, and low environmental impact. In hybrid systems, nanocellulose serves both as an active adsorbent and as a structural support, offering advantages such as high dispersibility, hydrophilicity, mechanical strength, and adaptable morphology [36]. Their incorporation into composites enhances surface area and promotes stronger interactions between active sites and pollutants, resulting in improved adsorption performance [37]. However, unmodified nanocellulose shows limited efficacy, necessitating chemical functionalization such as TEMPO-mediated oxidation, esterification, or amination to improve adsorption efficiency, mechanical stability, and reusability [38]. Additionally, nanocellulose-based membranes exhibit suitable pore structures, antifouling behavior, and high selectivity toward heavy metals and organic contaminants, making them promising candidates for advanced water purification [39].

3.1 Smart Cellulose Composites

Smart stimuli-responsive adsorbents can switch their structure or surface chemistry when exposed to triggers such as pH, temperature, light, magnetic fields, or ions. This reversible behavior influences both adsorption kinetics and thermodynamics. Kinetic effects such as structural changes (e.g., swelling, pore opening, or surface charge switching) can alter diffusion rates of pollutants into the adsorbent [40–42].

When the material is in its "active" state, larger pore volume or increased hydrophilicity can increase mass-transfer rates and accelerate adsorption. In the "inactive" state, collapsed chains or reduced surface accessibility slow down diffusion and reduce the rate constants. Thermodynamic effects, such as stimuli-induced changes in functional group availability or charge distribution, can modify binding energies between adsorbent and pollutant. This influences the equilibrium constant (K), meaning adsorption capacity may increase or decrease depending on whether the stimulus favors stronger or weaker interactions. Because the response is reversible, the system can shift between thermodynamically favorable and less favorable states without permanently altering the material. Overall, the controllable and reversible nature of these adsorbents allows external stimuli to adjust adsorption rate, capacity, and equilibrium behavior in real time [43–46]. A key advantage is their easy recovery by simply altering the applied stimulus, which supports recyclability and cost-effectiveness. Their high water retention capacity enhances contaminant interaction, while their mechanical strength allows multiple regeneration cycles without structural degradation [47].

3.1.1 Applications of Smart Cellulose Adsorbents in Water Treatment

pH-Stimuli Responsive Nano-Cellulose Adsorbents

pH-responsive nanocellulose composites are smart materials whose physicochemical properties can reversibly change with solution pH [48]. Typically, they are synthesized by grafting or integrating polyelectrolytes containing ionizable acidic and basic moieties into the cellulose matrix [40]. These functional groups undergo protonation and deprotonation in response to pH variations, leading to changes in surface charge, hydrophilicity, and polymer conformation [49,50]. Such transitions can manifest as swelling, deswelling, chain collapse, or extension, which directly influence adsorption behavior [40,42]. These pH-induced structural and conformational changes have been demonstrated in several studies where smart pH-responsive cellulose composites were synthesized for water treatment applications. In water remediation, pH-responsive nano-cellulose composites have demonstrated efficient removal of various pollutants, including dyes [40,41], oil/water separation [42], inorganic ions [51], fertilizer [52] (Table 2). Tian et al. [41] produced lysine-grafted porous cellulose foams incorporating glycidyl methacrylate, which provided amino and carboxyl groups responsible for pH responsiveness. The resulting Cell-g-PGMA-Lys adsorbent showed high capacities for removing both cationic methylene blue (1077.9 mg/g) and anionic reactive brilliant red X-3B (1210.7 mg/g) from wastewater. The kinetic and isothermal adsorption proved that dyes have been adsorbed in a single layer on Cell-g-PGMA-Lys, depending on the electrostatic interaction between the adsorbent membrane and adsorbate material. Similarly, Cheng et al. [42] developed two cellulose-based membranes with reversible pH-responsive wettability by grafting acrylamide and acrylic acid onto eucalyptus pulp, enabling effective oil–water separation due to their hydrophilic or hydrophobic behavior under different pH conditions.

Table 2: Applications of the stimuli-responsive cellulose composites in water remediation.

Analyte	Class of Analyte	Stimuli-Responsive Composite	Stimulus	Performance Parameters	Reference
Methylene Blue and Acid Orange II	Anionic and cationic dyes	Carboxymethyl cellulose/Chitosan hydrogel	pH	Maximum adsorption was 100 mg/g for Acid Orange II at pH_2 within five cycles, having a desorption rate higher than 90%. At pH 11, and 20 mg/g for Methylene Blue, having desorption rate reaching 95%	[40]

(Continued)

Table 2 (continued)

Analyte	Class of Analyte	Stimuli-Responsive Composite	Stimulus	Performance Parameters	Reference
Methylene blue and Brilliant red X-3B	Dyes	pH-responsive L-lysine-grafted cellulose porous foams	pH	Maximum dye adsorption capacity of 1077.9 mg/g and 1210.7 mg/g, for methylene blue and brilliant red X-3B, respectively	[41]
Oil-water separation	Hydrophilic-hydrophobic surface	Grafted polyacrylic acid (PAA) and grafted polyacrylamide (PAM) onto eucalyptus pulp cellulose.	pH		[42]
Methyl violet and methylene blue	Dyes	Cellulose micro-filaments/poly(N-Isopropylacrylamide-*co*-acrylic acid) spheres	PH and temperature	Adsorption capacities of 840.3 mg/g and 497.5 mg/g for methyl violet and methylene blue, respectively	[47]
Methylene blue	Organic dyes	Hydrogel result from reacting of activated carboxymethyl cellulose nanocrystals with l-cysteine generating amide bonds.	Redox-responsive hydrogel	Adsorption capacity of reached 756 mg/g at pH 11	[49]
Nitrate ions (NO_3^-)	Inorganic ions	Cellulose nanocrystals (CNCs)-grafted and block copolymers of 2-dimethylaminoethyl methacrylate	PH and temperature		[51]
Urea	Fertilizer	pH-responsive nano-cellulose/sodium alginate/MOFs	pH	Water adsorption of 100 mL/g and Surface area of 45.25 m^2/g	[52]
Oil-water separation	Hydrophilic-hydrophobic surface	Grafted N-isopropylacrylamide onto bagasse pulp	Temperature		[53]
Crude oil	Hydrophilic-hydrophobic surfacel	Exfoliated bentonite (BTex) and Ti_3C_2 MXene with carboxylated cellulose nanofibers (CNF-C)	Temperature	Maximum adsorption capacity of 48 mg/g of crude oil within 25 s under solar illumination	[54]
Lead Pb(II) ions	Heavy metals	Microfibrillated cellulose-based composite beads	pH and temperature	Adsorption capacity of 171.2 mg/g	[55]
Gold Au^{3+} ions	Heavy metals	Thiacrown ether-combined with thermo-stimuli responsive *N*-isopropylacryl-amide (NIPAM)	Temperature	Maximum adsorption capacity of 141.82 mg/g	[56]
Methyl orange, naphthol green B, and methyl blue	Dyes	CO_2-stimuli responsive cellulose nanofibril aerogel	CO_2	Maximum adsorption capacities of 892.9, 621.1, and 598.8 mg/g for methyl orange, naphthol green B, and methyl blue, respectively	[57]

(Continued)

Table 2 (continued)

Analyte	Class of Analyte	Stimuli-Responsive Composite	Stimulus	Performance Parameters	Reference
Nitrate ions (NO_3^-)	Inorganic ions	Block copolymers of dimethylamino-ethyl methacrylate (DMAEMA) and N-isopropylacrylamide (NIPAAm)/CNFs	CO_2 and temperature	Maximum Adsorption capacity of 490 mg/g	[58]

Thermo-Stimuli Responsive Nanocellulose Adsorbents

Thermo-responsive cellulose composites exhibit reversible physicochemical transitions in response to temperature changes [59]. These materials possess a critical solution temperature (CST), most commonly a lower critical solution temperature (LCST), below which they remain hydrophilic and water-swollen, and above which they become hydrophobic due to phase separation [53]. Thermo-responsive cellulose adsorbents have shown strong potential in oil–water remediation. Chen et al. [53] developed cellulose-g-PNIPAAm by grafting N-isopropylacrylamide onto bagasse pulp, resulting in a composite whose wettability changes with temperature. At 25°C it is hydrophilic due to hydrogen bonding with water, while at 45°C intra-molecular bonding makes it hydrophobic, allowing oil to permeate and rejecting water. The material maintained stable performance over five reuse cycles. Additionally, dual thermo-/pH-responsive cellulose composites have also proven effective. The thermo-responsive behavior of cellulose-g-PNIPAAm arises from temperature-dependent changes in hydrogen bonding within the PNIPAAm chains. At lower temperatures (around 25°C), the chains adopt a loosely coiled structure and form hydrogen bonds with surrounding water molecules, giving the material a hydrophilic surface. When the temperature rises to about 45°C, intramolecular hydrogen bonding between the C=O and N–H groups becomes dominant, causing the chains to collapse into a compact conformation. This reduces their ability to interact with water, switching the material's surface from hydrophilic to hydrophobic.

Recent studies have focused on multi-responsive cellulose-based systems capable of reacting to multiple environmental stimuli. Tang et al. [54] developed dual pH- and temperature-responsive CNC composites for controllable oil–water emulsion stabilization. The C/BTex/Ti_3C_2 aerogel was fabricated by integrating low-cost exfoliated bentonite (BTex) and Ti_3C_2 MXene with carboxylated cellulose nanofibers (CNF-C) using an *in-situ* co-precipitation process followed by microwave hydrothermal treatment and solution impregnation. BTex played a key role in preventing Ti_3C_2 oxidation and improving the aerogel's structural integrity, mechanical strength, and adsorption performance. As a result, the CNF-C/BTex/Ti_3C_2 aerogel showed excellent structural, thermal, and chemical stability, strong hydrophobicity (water contact angle of 149°), and good mechanical resilience (recovering fully after 60% strain). These properties enabled high oil adsorption capacities of 46–90 times its weight. Additionally, its high photothermal efficiency (99% light absorption, surface temperature reaching 75.2°C under 1-sun irradiation) and notable thermal conductivity (104 mW/m·K) further enhanced its performance, allowing it to absorb up to 48 $mg \cdot g^{-1}$ of crude oil within 25 s under solar illumination. Li et al. [47] synthesized cellulose microfilament/poly(N-isopropylacrylamide-co-acrylic acid) spheres (MPNAA), which efficiently removed cationic dyes such as methyl violet and methylene blue. In this system, acrylic acid provided pH responsiveness, PNIPAAm contributed temperature sensitivity, and dye adsorption was promoted by hydrogen bonding between –COOH and $–NH_2$ functional groups. The resulting adsorbent exhibited a porous structure and surface functional groups capable of effectively complexing with Pb^{2+} ions. Moreover, its adsorption behavior was responsive to both temperature

and pH, showing noticeable changes when the Pb^{2+} solution conditions were adjusted between 30°C–45°C and pH 2.0–6.0.

In another study, Li et al. created eco-friendly microfibrillated cellulose beads (MCPAs) with dual responsiveness for efficient removal of lead ions from wastewater [55]. MCPAs were synthesized by simultaneous copolymerization and crosslinking of microfibrillated cellulose with monomers, producing adsorbents that respond to both pH and temperature. The optimal pH for Pb^{2+} removal was 6.0, and at this pH the adsorption and desorption kinetics and isotherms were assessed at 30°C and 45°C. The equilibrium data followed the Langmuir model, giving a maximum Pb^{2+} adsorption capacity of 171.2 mg/g at 45°C, while the adsorption kinetics were best described by the pseudo-second-order model. Desorption followed the Korsmeyer–Peppas model. Column experiments further showed a high continuous-flow adsorption capacity of 187.3 mg/g, confirming the strong performance of the MCPAs.

CO_2-Stimuli Responsive Nano-Cellulose Adsorbents

CO_2-responsive nano-cellulose adsorbents are smart materials whose physicochemical properties can be reversibly tuned by CO_2 bubbling, which induces protonation of basic groups such as amines under mild, green conditions [57]. This approach avoids secondary pollution and allows easy regeneration by removing CO_2 through heating or N_2 purging. For example, Yang et al. [58] synthesized a CO_2-responsive CNF aerogel from poly(methacrylic acid-co-2-(dimethylamino)ethyl methacrylate) and carboxylated CNFs, achieving high adsorption capacities for methyl orange, naphthol green B, and methyl blue (892.9, 621.1, and 598.8 mg/g, respectively) with stable performance over 20 regeneration cycles. Meanwhile, the kinetics and adsorption isotherms of the CO_2-responsive adsorbents followed the Freundlich isotherm and the pseudo-second-order model, respectively. These findings demonstrate the sustainability and reusability of CO_2-triggered cellulose composites for efficient dye removal from wastewater. Eskandari et al. [60] developed a dual CO_2- and thermo-responsive cellulose nanocrystal composite by grafting CNCs onto PDMAEMA-b-PNIPAAm copolymers (HOOC-poly(N-isopropylacrylamide)-b-poly(2-(dimethylamino)ethylacrylate)-$C_{12}H_{25}$(HOOC-PNIPAM-b-PDMAEA-$C_{12}H_{25}$) and HOOC-poly(2-dimethylamino)ethylacrylate)-b-poly(N-isopropylacrylamide)-$C_{12}H_{25}$(HOOC-PDMAEA-b-PNIPAM-$C_{12}H_{25}$) diblock copolymers synthesized via atom transfer radical polymerization. The PDMAEMA block imparted CO_2 sensitivity, while the PNIPAAm block provided temperature responsiveness. The copolymers exhibit CO_2-responsive behavior because CO_2 bubbling lowers the solution pH and protonates the PDMAEMA tertiary amine groups. Depending on the hydrophilic–hydrophobic block ratio, the free copolymers formed micelles or vesicles. CO_2-triggered nitrate removal was tested below and above the copolymers' cloud separation temperatures (40°C and 60°C). Copolymers with longer PDMAEMA blocks showed the highest nitrate adsorption capacity (490 mg/g) at temperatures below the CST, driven by electrostatic interactions. The CNC-grafted copolymers also demonstrated N_2-induced desorption, thermal responsiveness, and good filtration properties, enabling easy regeneration.

3.2 Nanocellulose-Based MOF Composites

Metal–organic frameworks (MOFs) are crystalline materials composed of metal ions coordinated with organic ligands, forming extended three-dimensional networks (Fig. 1) [61]. Their unique properties, including high surface area, tunable pore size and functionality, and excellent thermal and chemical stability, have made them highly attractive for water purification applications. Nevertheless, nanoscale MOF particles are prone to agglomeration, which diminishes their reactivity and overall performance. To address this challenge, *in situ* growth or *ex situ* incorporation of MOFs into abundant and low-cost cellulose-based supports has been proposed as an efficient approach to improve the stability and dispersion of MOF

species [62]. This hybridization not only enhances the intrinsic properties of MOFs but also extends the practical applications of cellulose–MOF composites in water treatment.

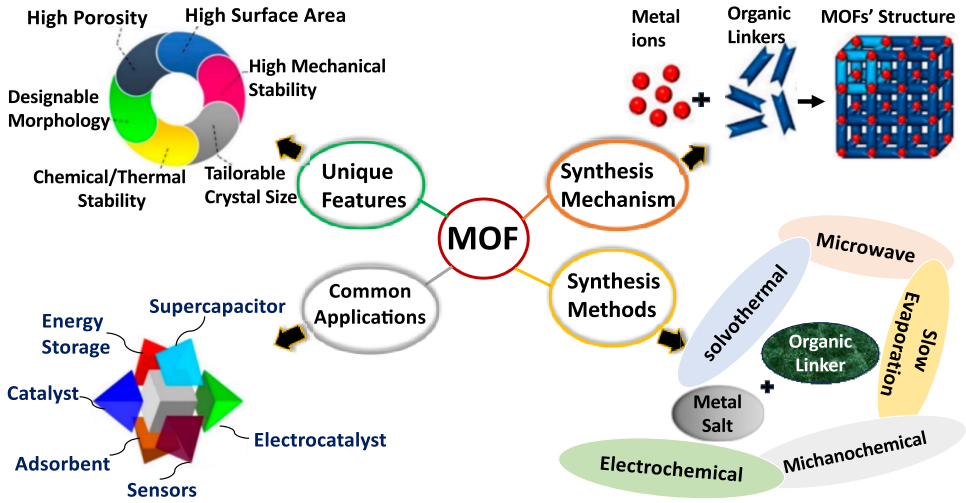

Figure 1: Schematic description of synthesis, mechanisms, features and general applications of metal organic frameworks (MOFs) [61].

For successful *in-situ* growth of metal–organic frameworks (MOFs) on cellulose fibers, surface modification is required to enhance metal ion coordination. Introducing carboxyl groups, such as through carboxymethylation, makes the cellulose surface anionic and supports strong MOF attachment [63]. The first example of this approach was reported in 2015, when TEMPO-oxidized cellulose nanofibers enabled MOF loading of up to 44%. It has also been noted that bio-MOFs can be produced directly using native or modified cellulose as the organic component [64]. A second method involves synthesizing cellulose materials first—such as aerogels, hydrogels, membranes, fabrics, or papers—and then incorporating preformed MOF crystals onto their surfaces. For instance, Zhu et al. prepared cellulose–MOF composites by attaching MOF particles to crosslinkable CNC and CMC [65]. Hybrid MOF aerogels were fabricated by first dispersing MOF particles with crosslinkable CNCs in water to create a stable colloidal suspension, which was then combined with an aqueous solution of crosslinkable carboxymethyl cellulose (CMC). The CNCs were modified with aldehyde groups (CHO–CNCs) and the CMC with hydrazide groups ($NHNH_2$-CMC), allowing hydrazone crosslinking upon mixing. This produced colloidally stable clusters where MOF particles were embedded within CNC–CMC crosslinked networks, mainly held together through physical entanglement and van der Waals forces. The suspension was subsequently frozen and freeze-dried to yield the hybrid MOF aerogels. Three types of MOFs—ZIF-8, UiO-66, and MIL-100(Fe)—were synthesized and successfully integrated into the cellulose aerogels, providing a range of particle sizes and functional properties. Because both the MOF particles and CNCs are rigid, steric hindrance limits the formation of CNC–CNC crosslinks. Therefore, the flexible $NHNH_2$-CMC component is essential to provide effective crosslinking and ensure the aerogels maintain strong mechanical integrity. Adsorption kinetics were evaluated by immersing the aerogels or corresponding MOF particles in 10 mL contaminant solutions (benzotriazole for ZIF-8, potassium dichromate for UiO-66, and Rhodamine B for MIL-100(Fe)) for set time intervals. The adsorption behavior over time was successfully described using the pseudo-second-order kinetic model. Both *in-situ* and *ex-situ* fabrication methods have since been widely reported [66–70].

Nanocellulose-based MOF composites have emerged as efficient and sustainable adsorbents for removing various contaminants from water, offering a promising alternative to conventional materials [69,70].

In these hybrids, cellulose nanoparticles serve as a flexible, lightweight, and multifunctional support, while MOFs contribute high porosity and large surface area. Adsorption can occur through several mechanisms, including hydrogen bonding, electrostatic attraction between charged species, ion exchange between adsorbent and pollutants, and complexation where chemical bonds form with contaminant molecules (as shown in Fig. 2) [71].

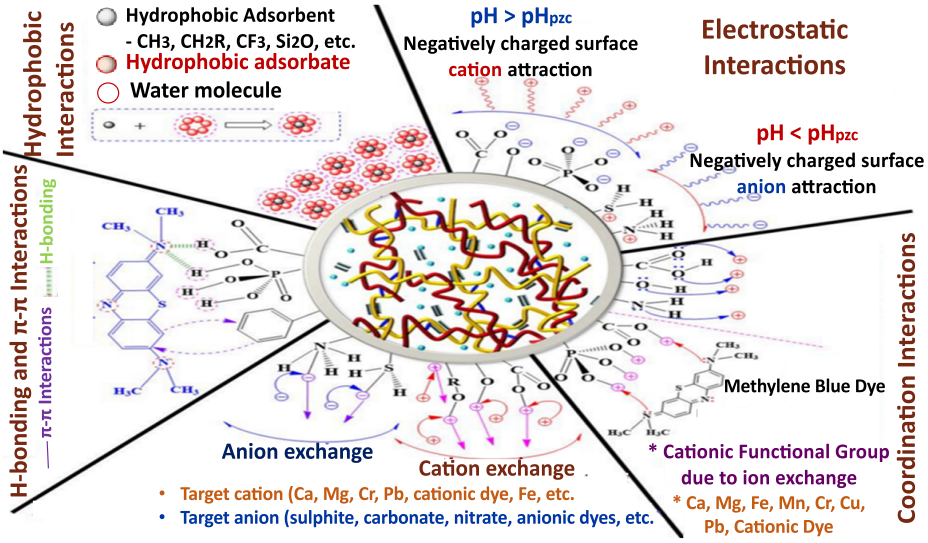

Figure 2: Interaction mechanisms between the adsorbent and pollutants in the water remediation using cellulose–based composites [71].

Dai et al. [72] developed a sustainable cellulose nanofiber aerogel functionalized with sulfonated covalent organic frameworks (SO_3H@COFs) for efficient Cd^{2+} removal from water. Using cellulose derived from biomass straws as a macroscopic scaffold, the one-step synthesis produced a hierarchical porous structure with abundant active sites and permeation channels. This design enabled high Cd^{2+} adsorption capacity through combined electrostatic attraction, coordination, and pore-driven mechanisms.

A ZIF-67-modified bacterial cellulose/chitosan (BC/CH) composite aerogel was synthesized via a simple process involving physical mixing, *in situ* growth, and lyophilization [73]. The resulting ZIF-67/BC/CH aerogel achieved a high ZIF-67 loading (46.1%) and a significantly increased surface area (268.7 m^2/g) compared to the pristine BC/CH aerogel (8.4 m^2/g). This composite effectively removed heavy metals and dyes from water, exhibiting high adsorption capacities of 200.6 mg/g for Cu^{2+} and 152.1 mg/g for Cr^{6+}. Flexible MOF-based aerogels were fabricated by *in situ* growth of ZIF-8 and UiO-66 nanoparticles on bacterial cellulose (BC), yielding composites with hierarchical porosity and macroscopic shapeability [74]. The resulting BC@ZIF-8 aerogels combined the high porosity of MOFs with the flexibility of BC, exhibiting low density (<0.03 g/cm^3), large surface area, and excellent mass transfer properties. The equilibrium adsorption of Cd^{2+} and Pb^{2+} on BC@ZIF-8 was approximately 220 and 390 mg/g, respectively. The adsorption kinetics were best described by the pseudo-second-order model. In simulated industrial wastewater, the composite achieved up to 81% Pb^{2+} removal, 1.2 times higher than that of pure ZIF-8 nanoparticles demonstrating superior adsorption efficiency. Functional MOFs and structural cellulose nanocrystals (CNCs) were integrated into a flexible, porous aerogel with a hierarchical architecture, without requiring chemical modification. The hybrid aerogel, fabricated via a simple sol–gel process followed by freeze-drying, demonstrated high efficiency in adsorbing Cr(VI) ions from contaminated water. The adsorption process was fitted with pseudo-second-order kinetic model. Tables 3–5 summarize a comparison

between different MOF-cellulose adsorbents for the removal of heavy metals, dyes and pharmaceuticals from the contaminated water.

Table 3: A comparison of different MOF–cellulose adsorbents for the removal of heavy metal ions.

Adsorbent	Heavy Metal Ion	Time and Temperature of Adsorption	Adsorption Capacity	Reference
Uio-66/CNFs/carboxy methyl cellulose Aerogel	Cr(VI)	The adsorption was conducted over 24 h without any agitation	Maximum adsorption capacity of 18 mg/g	[65]
ZIF/Cellulose Paper	Pb(II), Cd(II), Cu(II), Co(II), Fe(II)	12 h at 25°C	Maximum adsorption capacity of 261 mg/g for Pb(II), 143 mg/g for Cd(II), 143 mg/g for Cu(II), 350 mg/g for Co(II), 354 mg/g for Fe(II)	[68]
Cellulose nanofiber aerogel functionalized with sulfonated covalent organic frameworks (SO_3H@COFs)	Cd(II)	24 h at 55°C and pH 6	Maximum adsorption capacity of 50.71 mg/g	[72]
ZIF-67/BC/CH aerogel	Cu(II), Cr(VI)	24 h at 25°C	Maximum adsorption capacity of 200 mg/g for Cu(II), and 152 mg/g for Cr(VI)	[73]
BC/ZIF–8 aerogel	Pb(II), Cd(II)	12 h at 25°C	Maximum adsorption capacity of 380 mg/g for Pb(II)and 220 mg/g for Cd(II)	[74]
MCNC/Zn–BTC Composite	Pb(II)	0.5 h at 25°C	Maximum adsorption capacity of 558 mg/g	[75]
UiO–66–NH2/CA aerogel	Pb(II), Cu(II)	32 h at 25°C	Maximum adsorption capacity of 89 mg/g for Pb(II) and 39 mg/g for Cu(II)	[76]
ZIF-8/CA aerogel	Cr(VI)	2 h at 25°C	Maximum adsorption capacity of 28 mg/g	[77]
ZIF-8/CNF/cellulose foam	Cr(VI)	15 s at 25°C	Maximum adsorption capacity of 36 mg/g	[78]

Table 4: A comparison of different MOF–cellulose adsorbents for the removal of dyes.

Adsorbent	Dye	Adsorption Capacity	Reference
MIL-100(Fe)/CNFs/carboxy methyl cellulose Aerogel	Rhodamine B		[65]
ZIF-8/TEMPO-oxidized CNFs aerogels ZIF-8 crystals (Zn-MOFs (where, zinc as metal ion and benzene-1,3-dicarboxylic acid as the organic linker)	Rhodamine B	Adsorption capacity of 83.3 mg/g	[79]
Fe-MOF and cellulose-based composite aerogels	Congo Red dye	Adsorption capacity of 280.3 mg/g	[80]
UiO-66–nanocellulose aerogel (UiO-66 (Universitetet i Oslo) is MOF made up of $[Zr_6O_4(OH)_4]$ clusters with 1,4-benzodicarboxylic acid struts.	Anionic methyl orange and cationic methylene blue	Maximum adsorption capacity of anionic methyl orange (71.7 mg/g) and cationic methylene blue (51.8 mg/g)	[81]

(Continued)

Table 4 (continued)

Adsorbent	Dye	Adsorption Capacity	Reference
A mixture of cationic (Co-MOF-based zeolitic imidazolate frameworks) ZIF-67 MOF, anionic HKUST-1 MOF (The HKUST-1 MOF is made of dimeric metal units connected by benzene-1,3,5-tricarboxylate linker molecules) and CNFs hydrogel	Anionic methyl orange	Adsorption capacity of 49.2 mg/g	[82]

Table 5: A comparison of different MOF–cellulose adsorbents for the removal of pharmaceuticals.

Adsorbent	Pharmaceutical	Adsorption Capacity	Reference
Zwitterionic Cu-Zn-MOF/CNF aero-beads, combined binary ZIF-67 MOF and HKUST-1 MOF components	Anionic pharmaceutical (diclofenac)	Maximum adsorption capacity of 121.2 mg/g	[82]
Binary Ni-Co-MOFs/carboxymethyl cellulose (CMC) aerogel	Tetracycline hydrochloride	Maximum adsorption capacity of 625 mg/g	[83]
The *in-situ* growth of ZIF-67 into the polyaniline-regenerated cellulose aerogels	Tetracycline	Maximum adsorption capacity of 409.5 mg/g	[84]

3.3 Nanocelluose-Based Composites for Water Remediation

3.3.1 Removal of the Radioactive and Heavy Metal Ions

Heavy metal ions are toxic, non-biodegradable pollutants commonly found in wastewater. Various treatment methods, including adsorption, precipitation, membrane filtration, flocculation, coagulation, sedimentation, and electro-precipitation have been employed for their removal. Among these, adsorption is particularly promising due to its high efficiency, low cost, and potential for regenerating and reusing adsorbents (as summarized in Table 6).

Nanocellulose-based materials have demonstrated significant potential for heavy metal ion adsorption. For instance, TEMPO-oxidized cellulose nanofibers (CNFs) derived from rice husk were used for the removal of Pb^{2+} and La^{3+} ions from contaminated water [85]. Among the tested forms, suspension, freeze-dried, and magnetic nanocomposite, the CNF suspension exhibited the highest adsorption capacities of 193.2 mg/g for Pb^{2+} and 100.7 mg/g for La^{3+} ions due to the electrostatic interaction between the positively charged heavy metal ions by the negatively charged carboxylate group ($–COO^-$) of the TEMPO-oxidized CNF. The CNF-metal complexes formed gels, allowing easy separation via gravity filtration. Furthermore, 90% of the lanthanum content could be recovered as lanthanum oxychloride through incineration of the CNF/$LaCl_3$ gel.

Covalently functionalized cellulose nanomaterials with EDTA and polyethylene amine (PEA) have also shown high adsorption capacities toward divalent metal ions, particularly Pb^{2+}, Cu^{2+}, and Cd^{2+} due to various active groups of EDTA and ($–NH_2$, –OH, C=C) in addition to the high surface area of cellulose nanomaterials (Fig. 3) [86]. Similarly, CNF-based foams crosslinked with citric acid via freeze-drying effectively removed Cr(III) ions from polluted water [87]. In this work, cellulose nanofibril (CNF) foams were prepared using citric acid, a bio-based tricarboxylic acid, as a crosslinker through freeze-drying. It is evaluated how varying citric acid levels and applying a post-heating treatment influenced crosslink formation. Increasing the citric acid content slightly enlarged the pore structure and lowered the activation energy for thermal degradation of amorphous cellulose. Heat treatment mainly affected the rate at which cellulose was released into water. The mechanical properties of the foams changed upon

wetting. For chromium adsorption, the foams followed a two-stage kinetic pathway involving pseudo-second-order behavior and intraparticle diffusion at neutral pH, consistent with reversible physisorption. Beyond their metal uptake capacity, the foams showed good water resistance, releasing only small amounts of cellulose through Fickian diffusion with an initial burst release. Cationic polyethyleneimine-functionalized carboxylated CNF beads (P/CMCNFs) achieved an exceptional adsorption capacity of 1302.3 mg/g for Cr(VI), along with excellent re-usability [88].

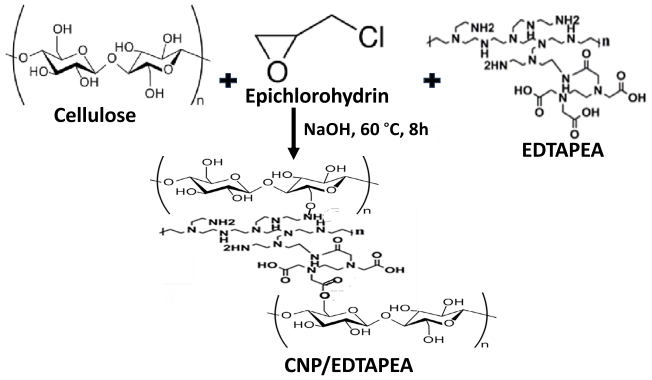

Figure 3: Schematic illustration of CNP/EDTA/PEI [86].

Recent studies have also focused on uranium recovery due to its relevance to nuclear energy and environmental remediation. Amidoximated CNFs prepared via acrylonitrile reaction and hydrolysis [89]. Cyanoethyl modification enabled cyanoethylated cellulose nanofibrils to be quickly exfoliated under mild shear conditions—such as simple shaking or homogenization—achieving nearly 90% conversion within 30 min and allowing the nanofibrils to be readily re-dispersed in a wide range of organic solvents. Following the hydrolysis of the cyanoethyl groups to amidoxime, the resulting amidoximated cellulose nanofibrils functioned as an environmentally friendly adsorbent, demonstrating exceptionally fast uranium uptake (under 5 min) and a high, reversible adsorption capacity of 1327 mg/g in aqueous systems.

Other CNF nanocomposites were used for the removal of Hg (II) [90,91], Cu(II) and Pb(II) [92–95].

Table 6: Cellulosic nanomaterials for the removal of radioactive and heavy metal ions.

Type of Nanocellulose	Composite	Metal Ion Removed	Adsorption Efficiency	Reference
Cellulose nanofibers (CNFs)	TEMPO-oxidized cellulose nanofibers (CNFs) derived from rice husk	Pb(II) and La (III) ions	193.2 mg/g for Pb(II) and 100.7 mg/g for La(III)	[85]
	Covalently functionalized cellulose nanomaterials with EDTA and polyethylene amine	Pb(II), Cu(II), and Cd(II)	393 mg/g for Pb(II); 139 for Cu(II), and 202 mg/g for Cd(II)	[86]
	CNF-based foams crosslinked with citric acid	Cr(III) ions		[87]
	Cationic polyethyleneimine-functionalized carboxylated CNF beads	Cr(VI) ions	1302.3 mg/g	[88]
	Amidoximated CNFs	Uranium ions	1327 mg/g	[89]
	Boron nitride quantum dots/CNFs	Hg(II) ions	314.5 mg/g	[90]
	CNFs/lysozyme nanofibrils	Hg(II) ions		[91]

(Continued)

Table 6 (continued)

Type of Nanocellulose	Composite	Metal Ion Removed	Adsorption Efficiency	Reference
Cellulose nanocrystals (CNCs)	CNFs crosslinked with acrylic acid aerogel	Cu(II) and Pb(II) ions	40.01 mg/g for Cu and 130.36 mg/g for Pb	[93]
	TEMPO-oxidized CNFs/metal–organic framework (MOF-808-ethylene diamine tetraacetic acid) aerogel	Cu(II) ions	300 mg/g	[94]
	TEMPO-oxidized CNFs/polyethyleneimine	Cu(II) ions		[95]
	Nanoscale zero-valent iron (nZVI) onto polydopamine-coated CNCs, forming	As (III/V)	333.3 mg/g for As(III) and 250 mg/g for As(V)	[96]
	Nanocomposite of CNCs hydrogel	Cu(II), Ni (II), Zn(II) and Cd(II) ions		[97]
	Nano-scale zero valent iron (nZVI)/CNCs	Ni(II) ions		[98]
Electrospun CNFs	ZIF-67/2-methylimidazole/cellulose acetate	Cr(VI) and Cu(II) ions	14.5 mg/g for Cr (VI) and 18.9 mg/g for Cu(II) ions	[99]
	Metal organic framework (MOF) [MIL-100(Fe)]/poly vinyl alcohol/cellulose acetate nanofibers	Cd(II) ions		[100]
	Electrospun cellulose acetate nanofiber membranes impregnated with cellulose nanocrystal (derived from areca nut husk), graphene oxide, along with an additional cross-linking modification with sericin	Cr, Pb, and Cu ions	A high flux rate of ~86–88 $L/m^{2/}h$ and metal retention of 93%, 90% and 84% for $PbCl_2$, $CrCl_3$, and $CuCl_2$ were achieved respectively	[101]
Bacterial nanocellulose (BNC)	BNC/$CaCO_3$ composite and carboxymethyl cellulose (CMC)/BNC composite	Cd(II) ions		[102]
	Poly(hexamethylenediamine-tannic acid)/bacterial cellulose	Cr(VI) ions	534.8 mg/g	[103]

Only a few studies have explored the use of cellulose nanocrystals (CNCs) for heavy metal ion removal. A mussel-inspired composite was developed by *in-situ* integrating nanoscale zero-valent iron (nZVI) onto polydopamine-coated CNCs, forming CNC/PDA/nZVI as an efficient adsorbent for arsenic (III/V) removal from groundwater [96]. The composite exhibited high adsorption capacities of 333.3 mg/g for As(III) and 250 mg/g for As(V), approximately ten times greater than that of pristine CNCs. The kinetic analysis showed that As removal is mainly governed by chemisorption. Isotherm results suggested that As(III) binds to the CNCs-PDA-nZVI surface in a uniform (homogeneous) manner, whereas As(V) interacts through varied (heterogeneous) sites. Overall, arsenic uptake occurs through a combination of adsorption-induced oxidation, coprecipitation, and the formation of inner-sphere surface complexes. Other studies include using of CNC composites for the removal of Cu(II), Ni(II), Zn(II) and Cd(II) ions [97,98].

Regarding the use of electrospun nanofibers, electrospun cellulose nanofibers incorporated with zeolitic imidazolate framework-67 (ZIF-67) enhanced metal ion removal performance. The *in-situ* integrated ZIF-67/2-methylimidazole/cellulose acetate (MIM/CA) composite achieved a significantly higher surface area

(463.1 m^2/g compared to 6.9 m^2/g for pristine MIM/CA) and improved adsorption capacities of 14.5 mg/g for Cr(VI) and 18.9 mg/g for Cu(II) ions [99]. The adsorption behavior follows pseudo-second-order kinetics. The mechanism involves both electrostatic interactions and ion-exchange processes, which together promote the efficient uptake of Cu(II) and Cr(VI). Additionally, the detection of Cr(III) after adsorption suggests that part of the Cr(VI) is reduced to Cr(III) during the process. Electrospun cellulose nanofiber composites were also used for removal of Cd, Cr, Pb, Ni, and Cu ions [100,101].

3.3.2 Removal of Dyes

Prolonged exposure to toxic dyes poses severe environmental and health risks, including respiratory issues, skin allergies, hormonal disruption, and certain cancers [104]. Consequently, dye removal from wastewater before discharge has become a critical environmental priority. Cellulosic nanomaterials have been widely investigated as efficient adsorbents for dye remediation. El-Sayed et al. [105] synthesized an anionic CNF derivative by grafting 3-aminopropyl sulfonic acid (3-APSA) onto TEMPO-oxidized CNFs, achieving a uniform morphology and enhanced methylene blue (MB) removal capacity of 526 mg/g—about 30% higher than that of ungrafted CNFs. The adsorption behavior of the adsorbents aligns well with the pseudo-second-order kinetic model and fits the Langmuir isotherm, indicating a good match with these models. Similarly, Mahardiani et al. [106] reported that Fe_3O_4-coated CNFs effectively adsorbed both cationic (MB, 9.973 mg/g) and anionic (Congo red, 9.711 mg/g) dyes, demonstrating the versatility of nanocellulose-based adsorbents in dye-contaminated water treatment.

From another perspective, Tran-Ly et al. developed a biohybrid foam composed of melanized cationic CNFs for bioinspired adsorption of the cationic dye crystal violet [107]. The CO_2-responsive composite demonstrated excellent recyclability, maintaining stable adsorption–desorption performance even after twenty regeneration cycles. Similarly, Zhu et al. [108] fabricated CNF/metal–organic framework (ZIF-8/CNF) membranes, which were pyrolyzed to form nanoporous N-doped carbon nanofilters (NCNFs). Methylene blue (MB) was used as a model pollutant to assess the catalytic degradation ability of NCNFs. The material showed outstanding performance, achieving 96% degradation of 10 mg/L MB within 15 min through PMS activation. Because the N-doped porous carbons are anchored onto CNF-based networks, the catalytic process and subsequent washing steps are straightforward. Radical-quenching tests indicated that MB degradation proceeds mainly through a non-radical pathway. Moreover, the NCNFs membrane exhibited excellent reusability after annealing and has strong potential as a catalytic filter for practical dye removal applications. Various other cellulose nanofiber-based derivatives and composites have been employed to remove different classes of dyes (Table 7). These systems incorporate CNF with materials such as Tara gum [109], PVA/magnetic nanorods [110], Pd nanoparticles (PdNPs)/nanozyme [111], and polyethylene imine (PEI) [112]. Additionally, metal-organic frameworks like ZIF-8 [113], and chitosan/alginate [114] have been utilized, alongside TEMPO-oxidized CNF functionalized with branched PEI [115].

Electrospun cellulose nanofiber membranes have been effectively utilized for the removal of various organic dyes (Table 7). Kumar et al. [116] fabricated an α-hematite/polyacrylonitrile/calcium carbonate/cellulose triacetate nanofiber membrane that achieved high adsorption efficiencies of 96% for methylene blue and 95% for methyl orange, while also removing Cu(II) and Pb(II) ions with efficiency 77% and 91%, respectively, due to the highly surface area and porosity of the electrospun CNF, in addition to the active groups of the polyacrylonitrile. Similarly, Ali et al. [117] demonstrated that polyaniline/β-cyclodextrin-modified electrospun cellulose acetate (CA-PANI/β-CD) nanofibers effectively adsorbed methylene blue (MB), confirming the versatility of electrospun cellulose-based materials in dye and metal ion remediation. The adsorption data were best described by the Langmuir isotherm, indicating monolayer adsorption, while the pseudo-second-order model accurately represented the adsorption kinetics of MB on CA-PANI/β-CD

nanofibers. In addition, the nanosorbent demonstrated good reusability, maintaining over 80% adsorption efficiency after three consecutive cycles. other electrospun CNF should activity in the removal of methylene bule and methyl orange dyes [118,119]

Relatively few studies have explored the use of cellulose nanocrystals (CNCs) and bacterial cellulose (BC) for dye removal (Table 7). Dhar et al. [120] synthesized CNC-supported zero-valent iron (ZVI) nanoparticles for efficient methylene blue adsorption from wastewater. The abundant hydroxyl groups on CNCs serve as effective anchoring sites, enabling simultaneous reduction and stabilization of CNC-supported ZVI particles. In this system, Na-CNCs act as corrosion inhibitors, helping the ZVI maintain its zero-valent state even after five days of air exposure. The resulting CNC-supported ZVI exhibit a narrow particle-size distribution and excellent dispersion stability in water. They efficiently degraded methylene blue and showed catalytic activity for converting 4-nitrophenol to 4-aminophenol, demonstrating their promise as safe and effective biocatalysts for wastewater treatment. Additionally, these Z(VI)-loaded CNCs displayed autonomous motion in peroxide solutions, with their speed and movement direction controllable through magnetic fields and pH gradients. Such tunable micromotors offer potential for future applications in sensing, imaging, and targeted drug delivery. Shanmugarajah et al. [121] utilized CNCs derived from oil palm biomass with an adsorption capacity of 50.91 mg/g for the methylene blue. Zhao et al. [122] developed CNCs/$Ti_3C_2T_x$ MXene/polyvinyl alcohol (PVA) composite for the removal of methylene blue with much higher efficiency 239.92 mg/g; the composite showed also removal efficiency of 45.25 mg/g for methyl orange.

Regarding the use of bacterial cellulose, Thorat et al. [123] developed a cationic bacterial cellulose/polyethyleneimine (PEI-BC) composite that effectively removed reactive red 120 (300.3 mg/L at pH 3) and Congo red (515.46 mg/L at pH 6), demonstrating a strong potential of BC-based adsorbents for dye remediation, due to the high crystallinity and the positively charged bacterial cellulose that efficiently adsorbed the negatively charged dyes, in addition to the active groups of polyethyleneimine. The adsorption of both anionic dyes followed pseudo-second-order kinetics, while the Langmuir isotherm provided the best fit for the equilibrium data. The PEI-BC adsorbent also demonstrated strong reusability, maintaining over 90% removal efficiency after four adsorption–desorption cycles. In addition, antibacterial tests against *E. coli* and *S. aureus* confirmed that the material exhibits notable bactericidal activity.

Table 7: Cellulosic nanomaterials for the removal of different types of dyes.

Type of Nanocellulose	Adsorbent	Dyes	Adsorption Capacity	Reference
Cellulose nanofibers (CNFs)	CNFs grafted with β-cyclodextrin aerogel	Methylene blue	3.46 mg/g	[92]
	Grafted 3-aminopropyl sulfonic acid (3-APSA) onto TEMPO-oxidized CNFs	Methylene blue	526 mg/g	[105]
	Fe_3O_4-coated CNFs	Methylene blue (MB) and Congo red (CR)	9.973 mg/g for cationic MB and 9.711 mg/g for anionic CR	[106]
	Melanized cationic CNFs foam	Crystal violet	0.5 mg/mg	[107]
	N-doped carbon nanofilters of ZIF-8/CNF) membranes	Methylene blue		[108]
	CNFs/Tara gum (TG) composite hydrogel	Methylene blue	13.7 mg/g	[109]
	CNFs/PVA magnetic beads	Cationic and anionic dyes		[110]
	Pd nanoparticles (PdNPs)/CNFs nanozyme	Methylene blue		[111]
	Polyethyleneimine (PEI)/CNFs cryogel	Methyl orange	500 mg/g	[112]

(Continued)

Table 7 (continued)

Type of Nanocellulose	Adsorbent	Dyes	Adsorption Capacity	Reference
	MOF (ZIF-8)/pomelo peel CNFs(PPCNFs) membranes	Methyl blue, Methyl violet, Malachite Green, and Rhodamine 6G		[113]
	(2,2,6,6-Tetramethyl piperidin-1-yl)oxyl (TEMPO)-oxidized cellulose nanofibers (TOCNF)/branched polyethylenimine 25 kDa (bPEI)	Naphthol Blue Black, Blue R, Orange II Sodium Salt, Brilliant Cibacron and Brilliant Yellow		[114]
	Chitosan/alginate/cellulose nanofibers bioadsorbent	Eriochrome Black-T	2297 mg/g	[115]
Electrospun CNFs	α-hematite/polyacrylonitrile/calcium carbonate/cellulose triacetate nanofiber membrane	Methyl orange		[116]
	polyaniline/β-cyclodextrin-modified electrospun cellulose acetate (CA-PANI/β-CD) nanofibers	Methylene blue		[117]
	ZIF-67/rice straw-derived cellulose acetate electrospun nanofiber mats	Methyl orange	11.20 mg/g	[118]
	Electrospun cellulose acetate/activated carbon composite modified by EDTA (rC/AC-EDTA)	Methylene blue		[119]
Cellulose nanocrystals (CNCs)	CNC-supported zero-valent iron (ZVI) nanoparticles	Methylene blue		[120]
	CNCs derived from oil palm biomass	Methylene Blue	50.91 mg/g	[121]
	CNCs/$Ti_3C_2T_x$ MXene/polyvinyl alcohol (PVA) composite	Methylene blue (MB) and Methyl orange (MO)	239.92 mg/g for MB and 45.25 mg/g for MO	[122]
Bacterial nanocellulose (BNC)	Cationic bacterial cellulose/polyethyleneimine (PEI-BC) composite	Reactive red and Congo red		[123]
	Cross-linked poly(2-methacryloyloxyethyl phosphorylcholine) (PMPC)/bacterial nanocellulose (BNC) zwitterionic nanocomposite membranes	Methylene blue and Methyl orange	4.4–4.5 mg/g	[124]

3.3.3 Removal of Oils

Wastewater from the petroleum industry contains high concentrations of crude oil and organic pollutants that pose serious risks to the environment, agriculture, and aquatic life. Effective treatment of such wastewater requires membranes with strong resistance to organic solvents. Bhuyan et al. [125] developed nanocomposite membrane using recycled materials from cellulosic paper and poly(ethylene terephthalate) (PET) waste. Cellulose nanofibers (CNFs) isolated from paper were blended with PET to form a porous CNF/PET membrane capable of separating synthetic crude oil–in–water emulsions. The membrane achieved over 97% removal of organic contaminants and a permeability of 98 $L/m^2 \cdot h$ under 1.5 bar pressure. Additionally, coating the membrane surface with carbon dot–rooted graphene oxide imparted antimicrobial properties. A nanocomposite membrane was developed using PET as the polymer matrix and CNF as a reinforcing additive. The material was engineered to be superhydrophilic and resistant

to organic solvents. A water-based phase inversion method was used to convert the composite into a porous membrane. This nanocomposite membrane, derived from water-processable materials, is intended for treating petroleum-industry wastewater. Additionally, a novel carbon-dot–assisted coating technique was used to anchor graphene oxide onto the membrane surface, providing antimicrobial activity and reducing biofouling. Huang et al. [126] addressed the limitations of conventional oil adsorbents by developing durable, hydrophobic cellulose nanofiber (CNF) composite aerogels for efficient oil/water separation. Using tannic acid (TA) as a molecular bridge between MOFs and CNF, the resulting aerogels exhibited improved pore structure, mechanical strength, and thermal stability. Further surface modification with methyltrimethoxysilane (MTMS) enhanced hydrophobicity (water contact angle of 133.9°) and boosted oil adsorption capacity (21.14–44.05 g/g). The optimized aerogels maintained 98.61% separation efficiency after 10 reuse cycles, demonstrating excellent durability and reusability. Additional research on oily wastewater remediation has explored CNF composites incorporating MOF (UiO-66-NH_2)/PVA [127] and silica nanoparticles/polyurethane [128]. Similarly, electrospun cellulose acetate nanofiber-based composites have demonstrated effectiveness in oil-water separation [129,130].

In addition to nanofibers, cellulose nanocrystals (CNCs) have been utilized in various composite configurations for oil–water removal [131–133], as summarized in Table 8. For example, Wang et al. [131] developed a hybrid membrane composed of CNCs, hydrolyzed electrospun polyacrylonitrile (H-PAN) nanofibers, cationic polyethyleneimine (PEI), and anionic silica (SiO_2) particles. In this study, cellulose nanocrystals (CNC) were used to reinforce hierarchical polyacrylonitrile (PAN) nanofibrous membranes. Hydrolysis of electrospun PAN (H-PAN) enabled hydrogen bonding with CNC and introduced reactive sites for grafting cationic polyethyleneimine (PEI). Subsequent adsorption of anionic silica (SiO_2) produced CNC/H-PAN/PEI/SiO_2 hybrid membranes with enhanced swelling resistance (swelling ratio of 6.7 vs. 25.4 for CNC/PAN). The resulting hydrophilic membranes feature highly interconnected channels, maintain mechanical and structural integrity, and allow regeneration and repeated use. Wettability and oil-in-water emulsion tests confirmed excellent oil rejection and separation efficiency compared to unmodified PAN membranes. This composite membrane demonstrated efficient separation of oils from aqueous solutions, highlighting the potential of CNC-based hybrids for oily wastewater treatment. A SiO_2 layer can be deposited on CNC/H-PAN nanofiber membranes using polyethyleneimine (PEI), which minimizes swelling. This stable coating also enhances surface cleanability by providing an anti-fouling effect.

Table 8: Cellulosic nanomaterials for the removal of oil from water/oil mixtures.

Type of Nanocellulose Material	Adsorbent	Type of Pollutant	Adsorption Efficiency	Reference
Cellulose nanofibers (CNFs)	CNF/poly(ethylene terephthalate) (PET) membrane	Crude Oil	97%	[125]
	Tannic acid (TA) as a molecular bridge between MOFs and CNF, the resulting aerogel modified with methyltrimethoxysilane (MTMS) to enhance hydrophobicity	Oil	The optimized aerogels maintained 98.61% separation efficiency after 10 reuse cycles	[126]
	MOF (UiO-66-NH2) incorporated PVA/cellulose nanofibers composite aerogel	Oil–water separation and formaldehyde adsorption		[127]
	Hydrophobic silica nanoparticles/polyurethane/cellulose nanofibers (SPC-Sponge)	Highly viscous Crude oil spills		

(Continued)

Table 8 (continued)

Type of Nanocellulose Material	Adsorbent	Type of Pollutant	Adsorption Efficiency	Reference
Electrospun CNFs	Zwitterionic copolymer poly(sulfobetaine methacrylate-r-glycidyl methacrylate)-grafted onto electrospun cellulose acetate nanofibers	Oil/water mixtures	98%	[129]
	Electrospun cellulose acetate/nano-zeolite nanofibers membrane	Oil/water mixtures	97%	[130]
Cellulose nanocrystals (CNCs)	Hybrid membrane composed of CNCs, hydrolyzed electrospun polyacrylonitrile (H-PAN) nanofibers, cationic polyethyleneimine (PEI), and anionic silica (SiO_2) particles	Oil/water mixtures		[131]
	Cellulose nanocrystals nanocoating and nanopapers fabricated by vacuum-filtration	Crude oil		[132]
	CNCs based membrane functionalized by block copolymer (poly(N-isopropylacrylamide)-b-poly(N,N-dimethylaminoethyl methacrylate))	Oil	99.6%	[133]

In another study, filter paper coated with CNCs proved efficient for removing oil from oil-water emulsions [132]. Additionally, CNCs functionalized with a poly(N-isopropylacrylamide)-b-poly(N,N-dimethylaminoethyl methacrylate) block copolymer were used to fabricate membranes. These membranes exhibited high water flux and excellent oil removal efficiency [133].

3.3.4 Removal of Pharmaceuticals

The presence of pharmaceuticals in aquatic environments poses severe ecological and health risks, contributing to antibiotic resistance and disrupting reproductive and behavioral systems across ecosystems. Consequently, the remediation of pharmaceutical-contaminated water has become a critical environmental challenge (see Table 9). Komal et al. [134] developed a carboxylated graphene oxide/esterified CNF composite that efficiently adsorbed the antibiotics ofloxacin and ciprofloxacin, with capacities of 85.30 and 45.04 mg/g, respectively. The adsorption consistency and reusability of the nanocomposite were evaluated by desorbing the loaded drug using 0.2 M NaOH under magnetic stirring for 3 h, followed by thorough washing with distilled water to remove residual NaOH. Jin et al. [135] fabricated a cellulose nanocrystal/hydroxyapatite nanocomposite achieving 70.81% removal efficiency for chlortetracycline hydrochloride within 10 min, demonstrating the potential of CNC-based materials for pharmaceutical pollutant removal. The removal mechanism involves a combination of interactions, including van der Waals forces, electrostatic interactions, and hydrogen bonding.

Table 9: Cellulosic nanomaterials utilized for the removal of pharmaceuticals.

Type of Nanocellulose Material	Adsorbent	Type of Pollutant	Adsorption Efficiency	Reference
Cellulose nanofibers (CNFs)	Carboxylated graphene oxide/Esterified CNFs composite adsorbent	Antibiotics (Ciprofloxacin and Ofloxacin)		[134]
	Cellulose nanocrystal/hydroxyapatite nanocomposite	chlortetracycline hydrochloride	70.81%	[135]
Cellulose nanocrystals (CNCs)	Ti_3C_2Tx MXene/CNFs membrane	Antibiotic (Azithromycin)	99%	[136]
	Sulfated cellulose nanocrystals/microcrystalline cellulose (MCC) nanocomposite Membrane	Tetracycline hydrochloride	89%	[137]
	Covalently modified CNCs using dioctenyldimethyl succinic anhydride (DDSA) (hydrophobic surface) or using polydiallyl dimethyl ammonium chloride (PDMC) (cationic) surface)	Diclofenac or Estradiol		[138]

3.3.5 Removal of Organic and Inorganic Pollutants

Aquifers are increasingly polluted with organic and inorganic contaminants, posing serious ecological risks. Owing to their safety, biocompatibility, and excellent physicochemical properties, nanocelluloses have been widely explored for water remediation (Table 10). Herrera-Morales et al. [139] fabricated nanocellulose–block copolymer films composed of CNFs/poly(4-vinylpyridine-b-ethylene oxide) (P4VP–PEO) and alkoxysilane-modified CNFs (TMPES/CNFs–P4VP–PEO) for the removal of emerging organic contaminants, effectively adsorbing sulfamethoxazole (SMX) as a model compound. Adsorption studies at neutral pH showed a capacity of 0.014 mmol/g within 60 min, likely driven by π-π interactions between the pyridine groups and SMX's aromatic rings. The films demonstrated excellent reusability, with adsorbed SMX efficiently removed using 95% ethanol, and minimal loss of capacity over multiple cycles. These CNF/P4VP-PEO films offer an effective and reusable platform for water remediation of electron-deficient aromatic pollutants. Likewise, Mantripragada et al. [140] developed electrospun cellulose/cellulose acetate nanofiber membranes coated with soy protein for the adsorption of polyfluoroalkyl substances (PFAS, GenX), achieving a capacity of 1.1 mmol/g.

Table 10: Cellulosic nanomaterials for the removal of different pollutants.

Type of Nanocellulose Material	Adsorbent	Type of Pollutant	Adsorption Efficiency	Reference
	α-hematite/polyacrylonitrile/calcium carbonate/cellulose triacetate nanofibers	Cu(II), Pb(II), methyl orange, methylene blue	96%	[116]
	CNFs/poly(4-vinylpyridine-b-ethylene oxide) (P4VP–PEO) and alkoxysilane-modified CNFs (TMPES/CNFs–P4VP–PEO) film	Sulfamethoxazole		[139]

(Continued)

Table 10 (continued)

Type of Nanocellulose Material	Adsorbent	Type of Pollutant	Adsorption Efficiency	Reference
Cellulose nanofibers (CNFs)	Electrospun cellulose (CE)/cellulose acetate (CA) nanofibers with soy protein coating membranes	Organic pollutant Polyfluoroalkyl substances (PFAS) (GenX)		[140]
	Polydopamine-coated CNF/amyloid protein aerogel	Acriflavine, rhodamine blue, crystal violet), Cu(II), Pb(II)], and organic compounds (ibuprofen, atrazine, bisphenol A		[141]
	TEMPO-oxidized CNF/natural rubber aerogels	Methylene blue, Cu(II), and oil	90% for oil	[142,143]
	CNFs/monolithic γ-aluminum oxy-hydroxide (γ-AlOOH) aerogel	Azo dyes: methylene blue (MB) and crystal violet (CV), and heavy metal ions: lead [Pb(II)], uranium [U(VI)], and arsenic [As(III)]	94%	[144]
	Laccase immobilized on dopamine functionalized cellulose nanofibers/alginate composite hydrogel	Bisphenol A (BPA) (Organic pollutant)	98.7%	[145]
	Macroporous surface-quaternized cellulose nanofibers (Q-CNF)/nano-$La(OH)_3$ aerogels	Phosphate		[146]
	Tethered cellulose fibers with disulphide linkages (CNFs-S-S-CNFs)	Mixed pollutants Safranin O (SO) Dye, Hg(II) ions	100% for SO Dye at pH 6 and 100% for Hg(II) at pH 5.5	[147]
Electrospun CNFs	Cellulose acetate/polyvinylpyrrolidone cores and β-FeOOH@MIL-100(Fe) photocatalytic sheaths	Cr(VI), oils, and dyes	(99.7%) for Cr(VI), (99.5%) for oils, and (99.4%) for dyes	[148]
	Electrospun TiO_2-graphene oxide (GO)/polyacrylonitrile (PAN)-cellulose acetate (CA) [TiO_2-GO/PAN-CA] nanofiber mats	Mixed pollutants Organic contaminants (Methylene Blue) and nitrophenol reduction	97% for MB as an organic dye, and 96% for the nitrophenol conversion to aminophenol	[149]
	Silicotungstic acid ($H_4SiW_{12}O_{40}$)/cellulose acetate composite nanofibrous membrane	Mixed pollutants Photocatalytic degradation of Tetracycline (TC) (as pharmaceutical) and Methyl Orange (MO) dye	63.8% for TC, 94.6% for MO	[150]
	Wool keratin/dialdehyde CNC biocomposite	Crystal violet and Cd(II)		[151]

(Continued)

Table 10 (continued)

Type of Nanocellulose Material	Adsorbent	Type of Pollutant	Adsorption Efficiency	Reference
Cellulose nanocrystals (CNCs)	Nanobentonite/dialdehyde CNC/carboxymethyl chitosan aerogel	Bromophenol Blue and 20.93 $g \cdot g^{-1}$ for Direct Blue 6		[152]
	Zirconium-metal organic framework Zr-MOF (UiO-66-H2)/chitosan/cellulose nanocrystal (CS-CNC) hybrid aerogel	Herbicide Glyphosate		[153]
	Bacterial cellulose (BC)/polydopamine (PDA)/carboxylated cellulose nanocrystals (CCNC)	Mixed pollutants lead ion Pb (II), Methylene Blue (MB)		[154]
	Reduced graphene oxide-cellulose nanocrystals (rGCA)/ethylene-propylene-diene monomer (EPDM) (rGCA/EPDM) aerogel	Mixed pollutants Oil, Organic solvents		[155]
Bacterial nanocellulose (BNC)	Zwitterionic Ag_2O nanoparticles/bacterial cellulose aerogel	Mixed pollutants Methylene Blue, Oil		[156]
	Bacterial cellulose/TiO_2-ZnO nanocomposites	Mixed pollutants Oil, Microbial contaminants	99.25% for oil, and 92% for photocatalytic degradation	[157]
	Photothermal carbon aerogel of Polydopamine/Cu nanoparticles (CuNPs)/bacterial cellulose nanofibers	Solar-driven seawater desalination		[158]

3.3.6 Removal of Mixed Pollutants

Mixed pollutants pose significant environmental hazards, making the development of multifunctional purification systems a major research challenge. Nanocellulose-based materials have shown great promise in removing diverse contaminants simultaneously (see Table 10). Sorriaux et al. [141] fabricated a polydopamine-coated CNF/amyloid protein aerogel with a dual-network structure formed via periodate oxidation, which efficiently adsorbed dyes (e.g., acriflavine, rhodamine blue, crystal violet), heavy metals [Cu(II), Pb(II)], and organic compounds (ibuprofen, atrazine, bisphenol A). The aerogel achieved high removal efficiencies, 93.1% for crystal violet, 94.7% for Pb(II), and 91.7% for bisphenol A within minutes. Moreover, the aerogel exhibits excellent reusability for Pb(II) ions, maintaining effective removal performance over multiple adsorption–desorption cycles. High porosity and abundant surface amino groups ($-NH_2$) facilitate the diffusion of Pb ions on the aerogel surface, following a pseudo-second-order kinetic model. Similarly, Lorevice et al. [142] developed TEMPO-oxidized CNF/natural rubber aerogels (TMI3) that showed high adsorption capacities of 334 mg/g for methylene blue and 420 mg/g for Cu(II). The aerogel demonstrated reuse efficiency of 66%–98% across multiple cycles and effectively removed Cu(II) from water at environmentally relevant concentrations (20–60 $\mu g \cdot L^{-1}$) without causing toxicity to *Daphnia similis*. Their earlier work demonstrated porous CNF/natural rubber latex foams capable of removing 90% of oil and 50 mg/g of oil/organic solvent, satisfying rapid and high-capacity absorption of oils and organic solvents (over 50 $g \cdot g^{-1}$ within 3 s) with outstanding reusability for up to 20 cycles [143]. Oher examples are given in Table 10 for removal of mixed pollutants such as mixed azo dyes, Pb ions, U(VI), As(III) [144], Bisphenol A [145], phosphate [146], Safranin O (SO) Dye and Hg(II) [147].

Regarding using the elctrospun nanofibers, Lu et al. [148] designed hybrid electrospun nanofiber membranes (ENMs) composed of deacetylated cellulose acetate/polyvinylpyrrolidone cores and β-FeOOH@MIL-100(Fe) photocatalytic sheaths, achieving exceptional removal efficiencies for Cr(VI) (99.7%), oils (99.5%), and dyes (99.4%). Additionally, the photocatalytic sheaths offer long-term reusability due to their intrinsic self-cleaning capability. Kumar et al. [116] reported α-hematite/polyacrylonitrile/calcium carbonate/cellulose triacetate nanofibers capable of removing both metal ions [Cu(II), Pb(II)] and dyes (methyl orange, methylene blue) with efficiencies up to 96%. Electrospun TiO_2-graphene oxide (GO)/polyacrylonitrile (PAN)-cellulose acetate (CA) [TiO_2-GO/PAN-CA] nanofiber mats was able to remove of 97% for MB as an organic dye, and 96% for the nitrophenol conversion to aminophenol [149] Silicotungstic acid ($H_4SiW_{12}O_{40}$)/cellulose acetate composite nanofibrous membrane showed good adsorption capacity towards photocatalytic degradation of Tetracycline (as pharmaceutical) and Methyl Orange dye (63.8% for Tetracycline and 94.6% for methyl orange) [150].

Regarding the use of CNC, Peiravi-Rivash et al. [151] reported a wool keratin/dialdehyde CNC biocomposite with outstanding adsorption capacities of 1166.67 mg/g for crystal violet and 695.56 mg/g for Cd(II), showing excellent recyclability. Sharma et al. [152] developed a nanobentonite/dialdehyde CNC/carboxymethyl chitosan aerogel. An ultralight aerogel was prepared by incorporating nano-bentonite into a dialdehyde nanocellulose and carboxymethyl chitosan network. The material exhibited outstanding adsorption for dyes, oils, and organic solvents, achieving rapid dye removal (up to 29.84 $g{\cdot}g^{-1}$ for Bromophenol Blue and 20.93 $g{\cdot}g^{-1}$ for Direct Blue 6 within 5 min) across a wide pH range, and absorbing oils/solvents up to 50 times its weight. The eco-friendly aerogel maintained high performance with only a slight decrease in adsorption after ten reuse cycles. Zirconium-metal organic framework Zr-MOF (UiO-66-NH2)/chitosan/cellulose nanocrystal (CS-CNC) hybrid aerogel composites was used to remove Glyphosate herbicide [153]. Composites from Bacterial cellulose/polydopamine/carboxylated cellulose nanocrystals were used to remove Mixed pollutants lead ion Pb (II) and Methylene Blue dye [154]. Reduced graphene oxide-cellulose nanocrystals (rGCA)/ethylene-propylene-diene monomer (EPDM) (rGCA/EPDM) aerogel was used to remove mixed pollutants oils and organic solvents [155].

Regarding using bacterial cellulose for removing mixed pollutants, Jiang et al. [156] prepared a zwitterionic Ag_2O nanoparticle/bacterial cellulose aerogel that effectively separated oil–water mixtures and photocatalytically degraded methylene blue, highlighting the multifunctionality of nanocellulose-based systems for mixed pollutant remediation. The prepared aerogel featured a stable 3D porous structure, ultralow density, and shape-recovery ability. Uniformly dispersed Ag_2O nanoparticles provided excellent photocatalytic degradation of methylene blue and high recyclability. Functionalization with zwitterionic silane compounds imparted superhydrophilicity, superoleophilicity, underwater superoleophobicity, and underoil superhydrophobicity, enabling highly efficient oil/water separation. Bacterial cellulose/TiO_2-ZnO nanocomposites were used to remove mixed pollutants oil and microbial contaminants [157]; Removal of 99.25% for oil and 92% by photocatalytic degradation could be achieved. Photothermal carbon aerogel of polydopamine/Cu nanoparticles (CuNPs)/bacterial cellulose nanofibers was prepared and used for the Solar-driven seawater desalination [158].

4 Conclusions and Future Perspectives

Cellulose, the most abundant natural biopolymer, possesses exceptional properties such as biocompatibility, biodegradability, non-toxicity, mechanical strength, and chemical tunability, making it an ideal eco-friendly material for water remediation. Its nanoscale forms (cellulose nanofibers, nanocrystals, bacterial cellulose, and electrospun nanofibers) offer high surface area, aspect ratio, and reactivity, enabling the design of advanced adsorbents and membranes. Owing to their hydrophilicity, nanocellulose-based

membranes also exhibit reduced fouling compared to synthetic polymer membranes. Various forms of cellulosic and nanocellulosic materials (membranes, aerogels, gels, suspensions, and smart composites) have been effectively applied for the removal of diverse pollutants through adsorption, photocatalysis, and responsive mechanisms. These sustainable materials present a promising alternative to petroleum-based polymers, minimizing environmental impact during production and disposal. Smart cellulose composites have reversible physicochemical properties that allow them to alter their structure or behavior when exposed to external stimuli such as temperature, light, pH, or redox conditions. Stimuli-responsive cellulose composites can be easily separated from treated water by simply altering external conditions, making them convenient to recover after use. This feature makes them cost-effective, eco-friendly, and recyclable adsorbents for water purification. In addition, these smart materials possess high mechanical strength, allowing them to withstand multiple regeneration cycles without notable structural degradation. Their strong water retention capability further enhances contaminant removal by ensuring sufficient contact time between pollutants and active adsorption sites. Cellulose-based MOF composites have demonstrated strong potential for removing various contaminants, making them promising alternatives to conventional adsorbents in water treatment. In these materials, cellulose serves as a flexible, lightweight, and multifunctional support, while the incorporated MOFs contribute high porosity and a large surface area for effective adsorption. In terms of future perspectives, most studies have focused on using cellulosic materials for the removal of heavy metals and water-soluble dyes, while comparatively limited research has addressed their modification for capturing hydrophobic pollutants such as pharmaceuticals, herbicides, organic dyes, synthetic insoluble effluents, and oils. Therefore, greater attention should be given to functionalizing cellulose with hydrophobic groups through chemical modification or composite formation to enhance its efficiency in removing non-polar contaminants. Beyond current advances, most studies have focused on introducing either anionic or cationic functional groups to cellulosic materials for removing pollutants of opposite charge. Future research should prioritize developing cellulose-based adsorbents containing both types of functional groups to enable simultaneous removal of pollutants with varying charges and enhance overall adsorption efficiency. In addition, integrating metal–organic frameworks (MOFs) with cellulose nanoparticles represents a promising direction for creating composites with higher surface area, lower density, and superior adsorption performance. Exploring different metal centers within MOFs could further improve the selectivity and efficiency of nanocellulose/MOF systems toward diverse contaminants. Moreover, comprehensive studies on the safety, stability, and biodegradability of cellulose derivatives and composites are essential to ensure environmental compatibility during use and after disposal. Finally, developing cost-effective and scalable synthesis routes remains a key challenge for the industrial commercialization of cellulose-based biosorbents.

Acknowledgement: The authors acknowledge the support of the National Research Centre (NRC) in Egypt by submitting the facilities required for completing this work.

Funding Statement: The authors received no specific funding.

Author Contributions: The authors confirm their contribution to the paper as follows: Study conception and design: Wafaa Abou-Elseoud, Mohammad Hassan; Writing—original Draft: Wafaa Abou-Elseoud, Mohammad Hassan; Writing—review and editing final manuscript: Wafaa Abou-Elseoud, Mohammad Hassan. All authors reviewed and approved the final version of the manuscript.

Availability of Data and Materials: The authors confirm that the data supporting the findings of this study are available within the article.

Ethics Approval: Not applicable.

Conflicts of Interest: The authors declare no conflicts of interest.

References

1. Boretti A, Rosa L. Reassessing the projections of the world water development report. npj Clean Water. 2019;2:15. doi:10.1038/s41545-019-0039-9.
2. Najib N, Christodoulatos C. Removal of arsenic using functionalized cellulose nanofibrils from aqueous solutions. J Hazard Mater. 2019;367:256–66. doi:10.1016/j.jhazmat.2018.12.067.
3. Ismael M, Mokhtar A, Adil H, Li X, Lü X. Appraisal of heavy metals exposure risks via water pathway by using a combination pollution indices approaches, and the associated potential health hazards on population, Red Sea State, Sudan. Phys Chem Earth Parts A B C. 2022;127:103153. doi:10.1016/j.pce.2022.103153.
4. Zhang X, Jiang J, Yuan F, Song W, Li J, Xing D, et al. Estimation of water footprint in seawater desalination with reverse osmosis process. Environ Res. 2022;204:112374. doi:10.1016/j.envres.2021.112374.
5. Jaiswal KK, Dutta S, Banerjee I, Pohrmen CB, Singh RK, Das HT, et al. Impact of aquatic microplastics and nanoplastics pollution on ecological systems and sustainable remediation strategies of biodegradation and photodegradation. Sci Total Environ. 2022;806(Pt 3):151358. doi:10.1016/j.scitotenv.2021.151358.
6. He J, Zhang Y, Ni F, Tian D, Zhang Y, Long L, et al. Understanding and characteristics of coagulation removal of composite pollution of microplastic and norfloxacin during water treatment. Sci Total Environ. 2022;831:154826. doi:10.1016/j.scitotenv.2022.154826.
7. Yin X, Tang S, Yong Q, Zhang X, Catchmark JM. Oriented 2D metal organic framework coating on bacterial cellulose for nitrobenzene removal from water by filtration. Sep Purif Technol. 2021;276:119366. doi:10.1016/j.seppur.2021.119366.
8. Huang X, Huang L, Babu Arulmani SR, Yan J, Li Q, Tang J, et al. Research progress of metal organic frameworks and their derivatives for adsorption of anions in water: a review. Environ Res. 2022;204(Pt D):112381. doi:10.1016/j.envres.2021.112381.
9. Zhao C, Liu G, Tan Q, Gao M, Chen G, Huang X, et al. Polysaccharide-based biopolymer hydrogels for heavy metal detection and adsorption. J Adv Res. 2023;44:53–70. doi:10.1016/j.jare.2022.04.005.
10. Musarurwa H, Tavengwa NT. Advances in the application of chitosan-based metal organic frameworks as adsorbents for environmental remediation. Carbohydr Polym. 2022;283:119153. doi:10.1016/j.carbpol.2022.119153.
11. Romita R, Rizzi V, Semeraro P, Gubitosa J, Gabaldón JA, Gorbe MIF, et al. Operational parameters affecting the atrazine removal from water by using cyclodextrin based polymers as efficient adsorbents for cleaner technologies. Environ Technol Innov. 2019;16:100454. doi:10.1016/j.eti.2019.100454.
12. Salehi E, Khajavian M, Sahebjamee N, Mahmoudi M, Drioli E, Matsuura T. Advances in nanocomposite and nanostructured chitosan membrane adsorbents for environmental remediation: a review. Desalination. 2022;527:115565. doi:10.1016/j.desal.2022.115565.
13. Misra N, Rawat S, Goel NK, Shelkar SA, Kumar V. Radiation grafted cellulose fabric as reusable anionic adsorbent: a novel strategy for potential large-scale dye wastewater remediation. Carbohydr Polym. 2020;249:116902. doi:10.1016/j.carbpol.2020.116902.
14. Rathnayake WSM, Karunanayake L, Samarasekara AMPB, Amarasinghe DAS. Fabrication and characterization of polypropylene–microcrystalline cellulose based composites with enhanced compatibility. In: 2019 Moratuwa Engineering Research Conference (MERCon); 2019 Jul 3–5; Moratuwa, Sri Lanka. p. 354–9. doi:10.1109/mercon.2019.8818914.
15. Kaur J, Sengupta P, Mukhopadhyay S. Critical review of bioadsorption on modified cellulose and removal of divalent heavy metals (Cd, Pb, and Cu). Ind Eng Chem Res. 2022;61(5):1921–54. doi:10.1021/acs.iecr.1c04583.
16. Saad HE, Hashem MA, El-Sayed YS, Gaber M, Abu El-Reash GM. Performance evaluation of cationic cellulose for anionic dyes adsorption from real wastewater and docking studies. Discov Chem. 2025;2(1):38. doi:10.1007/s44371-025-00123-0.
17. Ragab AH, Gumaah NF, El Aziz Elfiky AA, Mubarak MF. Exploring the sustainable elimination of dye using cellulose nanofibrils- vinyl resin based nanofiltration membranes. BMC Chem. 2024;18(1):121. doi:10.1186/s13065-024-01211-5.

18. Zhang J, Jiang F, Lu Y, Wei S, Xu H, Zhang J, et al. Lignin microparticles-reinforced cellulose filter paper for simultaneous removal of emulsified oils and dyes. Int J Biol Macromol. 2023;230:123120. doi:10.1016/j.ijbiomac.2022.123120.
19. Habibi Y, Lucia LA, Rojas OJ. Cellulose nanocrystals: chemistry, self-assembly, and applications. Chem Rev. 2010;110(6):3479–500. doi:10.1021/cr900339w.
20. Lavoine N, Desloges I, Dufresne A, Bras J. Microfibrillated cellulose–Its barrier properties and applications in cellulosic materials: a review. Carbohydr Polym. 2012;90(2):735–64. doi:10.1016/j.carbpol.2012.05.026.
21. Xie H, Du H, Yang X, Si C. Recent strategies in preparation of cellulose nanocrystals and cellulose nanofibrils derived from raw cellulose materials. Int J Polym Sci. 2018;2018(1):7923068. doi:10.1155/2018/7923068.
22. Islam MS, Rahaman MS, Yeum JH. Electrospun novel super-absorbent based on polysaccharide-polyvinyl alcohol-montmorillonite clay nanocomposites. Carbohydr Polym. 2015;115:69–77. doi:10.1016/j.carbpol.2014.08.086.
23. Tayeb AH, Amini E, Ghasemi S, Tajvidi M. Cellulose nanomaterials—binding properties and applications: a review. Molecules. 2018;23(10):2684. doi:10.3390/molecules23102684.
24. Sofla MRK, Brown RJ, Tsuzuki T, Rainey TJ. A comparison of cellulose nanocrystals and cellulose nanofibres extracted from bagasse using acid and ball milling methods. Adv Nat Sci Nanosci Nanotechnol. 2016;7(3):035004. doi:10.1088/2043-6262/7/3/035004.
25. Prasad Yadav T, Manohar Yadav R, Pratap Singh D. Mechanical milling: a top down approach for the synthesis of nanomaterials and nanocomposites. Nanosci Nanotechnol. 2012;2(3):22–48. doi:10.5923/j.nn.20120203.01.
26. Hassan M, Berglund L, Hassan E, Abou-Zeid R, Oksman K. Effect of xylanase pretreatment of rice straw unbleached soda and neutral sulfite pulps on isolation of nanofibers and their properties. Cellulose. 2018;25(5):2939–53. doi:10.1007/s10570-018-1779-2.
27. Chen Y, He Y, Fan D, Han Y, Li G, Wang S. An efficient method for cellulose nanofibrils length shearing via environmentally friendly mixed cellulase pretreatment. J Nanomater. 2017;2017(1):1591504. doi:10.1155/2017/1591504.
28. Tshikovhi A, Mishra SB, Mishra AK. Nanocellulose-based composites for the removal of contaminants from wastewater. Int J Biol Macromol. 2020;152:616–32. doi:10.1016/j.ijbiomac.2020.02.221.
29. Flauzino Neto WP, Mariano M, da Silva ISV, Silvério HA, Putaux JL, Otaguro H, et al. Mechanical properties of natural rubber nanocomposites reinforced with high aspect ratio cellulose nanocrystals isolated from soy hulls. Carbohydr Polym. 2016;153:143–52. doi:10.1016/j.carbpol.2016.07.073.
30. Novo LP, Bras J, García A, Belgacem N, da Silva Curvelo AA. A study of the production of cellulose nanocrystals through subcritical water hydrolysis. Ind Crops Prod. 2016;93:88–95. doi:10.1016/j.indcrop.2016.01.012.
31. Kusmono, Listyanda RF, Wildan MW, Ilman MN. Preparation and characterization of cellulose nanocrystal extracted from ramie fibers by sulfuric acid hydrolysis. Heliyon. 2020;6(11):e05486. doi:10.1016/j.heliyon.2020.e05486.
32. Amin KNM, Hosseinmardi A, Martin DJ, Annamalai PK. A mixed acid methodology to produce thermally stable cellulose nanocrystal at high yield using phosphoric acid. J Bioresour Bioprod. 2022;7(2):99–108. doi:10.1016/j.jobab.2021.12.002.
33. Kucińska-Lipka J, Gubanska I, Janik H. Bacterial cellulose in the field of wound healing and regenerative medicine of skin: recent trends and future prospectives. Polym Bull. 2015;72(9):2399–419. doi:10.1007/s00289-015-1407-3.
34. Hou Y, Duan C, Zhu G, Luo H, Liang S, Jin Y, et al. Functional bacterial cellulose membranes with 3D porous architectures: conventional drying, tunable wettability and water/oil separation. J Membr Sci. 2019;591:117312. doi:10.1016/j.memsci.2019.117312.
35. Vasanth Kumar U, Narayanasamy S, Uthandi S. Bacterial cellulose: a comprehensive review on biosynthesis, sustainable production, and multifaceted industrial applications. Food Bioprod Process. 2025;154:153–74. doi:10.1016/j.fbp.2025.08.013.
36. Qiu J, Li M, Ding M, Yao J. Cellulose tailored semiconductors for advanced photocatalysis. Renew Sustain Energy Rev. 2022;154(C):111820. doi:10.1016/j.rser.2021.111820.

37. El-Fattah WA, Guesmi A, Ben Hamadi N, Alayyafi AA, Shahat A. Novel composite based on cellulose nanomaterial for detection and selective removal of cadmium (II) ions from wastewater. Microchem J. 2024;198:110175. doi:10.1016/j.microc.2024.110175.
38. Iqbal D, Zhao Y, Zhao R, Russell SJ, Ning X. A review on nanocellulose and superhydrophobic features for advanced water treatment. Polymers. 2022;14(12):2343. doi:10.3390/polym14122343.
39. Rukaramato R, Babatunde D, Madanhire T, Mketo N, Magwa N. Nanocellulose-based materials for the removal of metal ions, pharmaceuticals, pesticides, dyes, and other pollutants from aqueous environments: a review. J Ind Eng Chem. 2025;150:265–99. doi:10.1016/j.jiec.2025.05.028.
40. Wang W, Hu J, Zhang R, Yan C, Cui L, Zhu J. A pH-responsive carboxymethyl cellulose/chitosan hydrogel for adsorption and desorption of anionic and cationic dyes. Cellulose. 2021;28(2):897–909. doi:10.1007/s10570-020-03561-4.
41. Tian X, Yang R, Chen T, Cao Y, Deng H, Zhang M, et al. Removal of both anionic and cationic dyes from wastewater using pH-responsive adsorbents of L-lysine molecular-grafted cellulose porous foams. J Hazard Mater. 2022;426:128121. doi:10.1016/j.jhazmat.2021.128121.
42. Cheng M, He H, Zhu H, Guo W, Chen W, Xue F, et al. Preparation and properties of pH-responsive reversible-wettability biomass cellulose-based material for controllable oil/water separation. Carbohydr Polym. 2019;203:246–55. doi:10.1016/j.carbpol.2018.09.051.
43. Khamis F, Hegab HM, Banat F, Arafat HA, Hasan SW. Comprehensive review on pH and temperature-responsive polymeric adsorbents: mechanisms, equilibrium, kinetics, and thermodynamics of adsorption processes for heavy metals and organic dyes. Chemosphere. 2024;349:140801. doi:10.1016/j.chemosphere.2023.140801.
44. Milster S, Chudoba R, Kanduč M, Dzubiella J. Cross-linker effect on solute adsorption in swollen thermoresponsive polymer networks. Phys Chem Chem Phys. 2019;21(12):6588–99. doi:10.1039/c8cp07601d.
45. Mahmood U, Alkorbi AS, Hussain T, Nazir A, Qadir MB, Khaliq Z, et al. Adsorption of lead ions from wastewater using electrospun zeolite/MWCNT nanofibers: kinetics, thermodynamics and modeling study. RSC Adv. 2024;14(9):5959–74. doi:10.1039/d3ra07720a.
46. Srivastava A, Srivastava N, Nayak R, Singh R. Kinetic and thermodynamic evaluation of adsorptive removal of lead(II) from aqueous solutions using Polypyrrole@$CoFe_2O_4$ nano-adsorbent. Prog React Kinet Mech. 2025;50:e006. doi:10.48130/prkm-0025-0006.
47. Li Y, Xiao H, Pan Y, Zhang M, Jin Y. Thermal and pH dual-responsive cellulose microfilament spheres for dye removal in single and binary systems. J Hazard Mater. 2019;377:88–97. doi:10.1016/j.jhazmat.2019.05.033.
48. Mohan T, Ajdnik U, Nagaraj C, Lackner F, Dobaj Štiglic A, Palani T, et al. One-step fabrication of hollow spherical cellulose beads: application in pH-responsive therapeutic delivery. ACS Appl Mater Interfaces. 2022;14(3):3726–39. doi:10.1021/acsami.1c19577.
49. Dubey N, Arora S. Surfactant assisted synthesis of pH responsive polyaniline-cellulose biocomposite for sensor applications. Polym Plast Technol Mater. 2021;60(10):1135–47. doi:10.1080/25740881.2021.1888985.
50. Gong Y, Mohd S, Wu S, Liu S, Pei Y, Luo X. pH-responsive cellulose-based microspheres designed as an effective oral delivery system for insulin. ACS Omega. 2021;6(4):2734–41. doi:10.1021/acsomega.0c04946.
51. Abousalman-Rezvani Z, Eskandari P, Roghani-Mamaqani H, Mardani H, Salami-Kalajahi M. Grafting light-, temperature, and CO_2-responsive copolymers from cellulose nanocrystals by atom transfer radical polymerization for adsorption of nitrate ions. Polymer. 2019;182:121830. doi:10.1016/j.polymer.2019.121830.
52. Wang Y, Shaghaleh H, Hamoud YA, Zhang S, Li P, Xu X, et al. Synthesis of a pH-responsive nano-cellulose/sodium alginate/MOFs hydrogel and its application in the regulation of water and N-fertilizer. Int J Biol Macromol. 2021;187:262–71. doi:10.1016/j.ijbiomac.2021.07.154.
53. Chen W, He H, Zhu H, Cheng M, Li Y, Wang S. Thermo-responsive cellulose-based material with switchable wettability for controllable oil/water separation. Polymers. 2018;10(6):592. doi:10.3390/polym10060592.
54. Tang R, Hu Y, Yan J, Xu S, Wang Y, Yan J, et al. Multifunctional carboxylated cellulose nanofibers/exfoliated bentonite/Ti_3C_2 aerogel for efficient oil adsorption and recovery: the dual effect of exfoliated bentonite and MXene. Chem Eng J. 2023;473:145412. doi:10.1016/j.cej.2023.145412.

55. Li Y, Xie D, Xiao J, Wu W, Zhang L, Xiao H, et al. Dual responsive copolymers-grafted microfibrillated cellulose composites for removing lead ions from aqueous solution. J Clean Prod. 2020;258:120867. doi:10.1016/j.jclepro.2020.120867.
56. Fissaha HT, Chung W, Gebremichael GT, Rajkamal A, Kim H, Parohinog KJ, et al. Selective and sustainable recovery of Au^{3+} through complexation-reduction capture and mechano-assisted release by thermo-responsive poly(N-isopropylacrylamide-co-15-thiacrown-4 ether)@SiO_2 nanoparticles. Chem Eng J. 2022;431:133698. doi:10.1016/j.cej.2021.133698.
57. Fan S, Chen J, Fan C, Chen G, Liu S, Zhou H, et al. Fabrication of a CO_2-responsive chitosan aerogel as an effective adsorbent for the adsorption and desorption of heavy metal ions. J Hazard Mater. 2021;416:126225. doi:10.1016/j.jhazmat.2021.126225.
58. Yang L, Zhan Y, Gong Y, Ren E, Lan J, Guo R, et al. Development of eco-friendly CO_2-responsive cellulose nanofibril aerogels as green adsorbents for anionic dyes removal. J Hazard Mater. 2021;405:124194. doi:10.1016/j.jhazmat.2020.124194.
59. Shi X, Lu W, Xue Y, Zhou H, Xue F, He H, et al. Design of thermo-responsive hyperbranched nanofibre-based adsorbent with high CO_2 adsorption capacity and analysis of its ultra-low temperature regeneration mechanism. Chem Eng J. 2021;424:130362. doi:10.1016/j.cej.2021.130362.
60. Eskandari P, Abousalman-Rezvani Z, Roghani-Mamaqani H, Salami-Kalajahi M. Carbon dioxide-switched removal of nitrate ions from water by cellulose nanocrystal-grafted and free multi-responsive block copolymers. J Mol Liq. 2020;318:114301. doi:10.1016/j.molliq.2020.114301.
61. Seidi F, Jouyandeh M, Taghizadeh M, Taghizadeh A, Vahabi H, Habibzadeh S, et al. Metal-organic framework (MOF)/epoxy coatings: a review. Materials. 2020;13(12):2881. doi:10.3390/ma13122881.
62. Tao Y, Du J, Cheng Y, Lu J, Min D, Wang H. Advances in application of cellulose—MOF composites in aquatic environmental treatment: remediation and regeneration. Int J Mol Sci. 2023;24(9):7744. doi:10.3390/ijms24097744.
63. Matsumoto M, Kitaoka T. Ultraselective gas separation by nanoporous metal-organic frameworks embedded in gas-barrier nanocellulose films. Adv Mater. 2016;28(9):1765–9. doi:10.1002/adma.201504784.
64. Vaidya LB, Nadar SS, Rathod VK. Biological metal organic framework (bio-MOF) of glucoamylase with enhanced stability. Colloids Surf B Biointerfaces. 2020;193:111052. doi:10.1016/j.colsurfb.2020.111052.
65. Zhu H, Yang X, Cranston ED, Zhu S. Flexible and porous nanocellulose aerogels with high loadings of metal-organic-framework particles for separations applications. Adv Mater. 2016;28(35):7652–7. doi:10.1002/adma.201601351.
66. Lu Y, Liu C, Mei C, Sun J, Lee J, Wu Q, et al. Recent advances in metal organic framework and cellulose nanomaterial composites. Coord Chem Rev. 2022;461:214496. doi:10.1016/j.ccr.2022.214496.
67. Abdelhamid HN, Mathew AP. Cellulose–metal organic frameworks (CelloMOFs) hybrid materials and their multifaceted applications: a review. Coord Chem Rev. 2022;451:214263. doi:10.1016/j.ccr.2021.214263.
68. Abdelhamid HN, Georgouvelas D, Edlund U, Mathew AP. CelloZIFPaper: cellulose-ZIF hybrid paper for heavy metal removal and electrochemical sensing. Chem Eng J. 2022;446:136614. doi:10.1016/j.cej.2022.136614.
69. Varghese AG, Paul SA, Latha MS. Remediation of heavy metals and dyes from wastewater using cellulose-based adsorbents. Environ Chem Lett. 2019;17(2):867–77. doi:10.1007/s10311-018-00843-z.
70. Du C, Zhang Z, Yu G, Wu H, Chen H, Zhou L, et al. A review of metal organic framework (MOFs)-based materials for antibiotics removal via adsorption and photocatalysis. Chemosphere. 2021;272:129501. doi:10.1016/j.chemosphere.2020.129501.
71. Akter M, Bhattacharjee M, Dhar AK, Bin Abdur Rahman F, Haque S, Rashid TU, et al. Cellulose-based hydrogels for wastewater treatment: a concise review. Gels. 2021;7(1):30. doi:10.3390/gels7010030.
72. Dai Y, Liu J, Zhao B, Qiu F, Tian Q, Xue S, et al. Self-assembled engineering construction of sustainable cellulose nanofibers aerogels and removal of cadmium (II) ion with spatial framework and permeation channels. Chem Eng Sci. 2026;319:122293. doi:10.1016/j.ces.2025.122293.
73. Li D, Tian X, Wang Z, Guan Z, Li X, Qiao H, et al. Multifunctional adsorbent based on metal-organic framework modified bacterial cellulose/chitosan composite aerogel for high efficient removal of heavy metal ion and organic pollutant. Chem Eng J. 2020;383:123127. doi:10.1016/j.cej.2019.123127.

74. Ma X, Lou Y, Chen XB, Shi Z, Xu Y. Multifunctional flexible composite aerogels constructed through *in-situ* growth of metal-organic framework nanoparticles on bacterial cellulose. Chem Eng J. 2019;356:227–35. doi:10.1016/j.cej.2018.09.034.
75. Wang N, Ouyang XK, Yang LY, Omer AM. Fabrication of a magnetic cellulose nanocrystal/metal–organic framework composite for removal of Pb(II) from water. ACS Sustainable Chem Eng. 2017;5(11):10447–58. doi:10.1021/acssuschemeng.7b02472.
76. Lei C, Gao J, Ren W, Xie Y, Abdalkarim SYH, Wang S, et al. Fabrication of metal-organic frameworks@cellulose aerogels composite materials for removal of heavy metal ions in water. Carbohydr Polym. 2019;205:35–41. doi:10.1016/j.carbpol.2018.10.029.
77. Bo S, Ren W, Lei C, Xie Y, Cai Y, Wang S, et al. Flexible and porous cellulose aerogels/zeolitic imidazolate framework (ZIF-8) hybrids for adsorption removal of Cr(IV) from water. J Solid State Chem. 2018;262:135–41. doi:10.1016/j.jssc.2018.02.022.
78. Ma S, Zhang M, Nie J, Tan J, Song S, Luo Y. Lightweight and porous cellulose-based foams with high loadings of zeolitic imidazolate frameworks-8 for adsorption applications. Carbohydr Polym. 2019;208:328–35. doi:10.1016/j.carbpol.2018.12.081.
79. Zhu L, Zong L, Wu X, Li M, Wang H, You J, et al. Shapeable fibrous aerogels of metal-organic-frameworks templated with nanocellulose for rapid and large-capacity adsorption. ACS Nano. 2018;12(5):4462–8. doi:10.1021/acsnano.8b00566.
80. Huang C, Cai B, Zhang L, Zhang C, Pan H. Preparation of iron-based metal-organic framework @cellulose aerogel by *in situ* growth method and its application to dye adsorption. J Solid State Chem. 2021;297:122030. doi:10.1016/j.jssc.2021.122030.
81. Wang Z, Song L, Wang Y, Zhang XF, Hao D, Feng Y, et al. Lightweight UiO-66/cellulose aerogels constructed through self-crosslinking strategy for adsorption applications. Chem Eng J. 2019;371:138–44. doi:10.1016/j.cej.2019.04.022.
82. KarzarJeddi M, Laitinen O, Mahkam M, Liimatainen H. Zwitterionic hybrid aerobeads of binary metal organic frameworks and cellulose nanofibers for removal anionic pollutants. Mater Des. 2020;196:109106. doi:10.1016/j.matdes.2020.109106.
83. Yang W, Han Y, Li C, Zhu L, Shi L, Tang W, et al. Shapeable three-dimensional CMC aerogels decorated with Ni/Co-MOF for rapid and highly efficient tetracycline hydrochloride removal. Chem Eng J. 2019;375:122076. doi:10.1016/j.cej.2019.122076.
84. Qun L, Yu H, Zeng F, Xiao L, Jing S, Hu X, et al. Polyaniline as interface layers promoting the *in-situ* growth of zeolite imidazole skeleton on regenerated cellulose aerogel for efficient removal of tetracycline. J Colloid Interface Sci. 2020;579:119–27. doi:10.1016/j.jcis.2020.06.056.
85. Zhan C, Sharma PR, He H, Sharma SK, McCauley-Pearl A, Wang R, et al. Rice husk based nanocellulose scaffolds for highly efficient removal of heavy metal ions from contaminated water. Environ Sci Water Res Technol. 2020;6(11):3080–90.
86. Alsaeedi H, Ahmad H, Altowairqi MF, Alhamed AA, Alsalme A. Covalently functionalized cellulose nanoparticles for simultaneous enrichment of Pb(II), Cd(II) and Cu(II) ions. Polymers. 2023;15(3):532. doi:10.3390/polym15030532.
87. da Silva DJ, Rosa DS. Chromium removal capability, water resistance and mechanical behavior of foams based on cellulose nanofibrils with citric acid. Polymer. 2022;253:125023. doi:10.1016/j.polymer.2022.125023.
88. Kim Y, Park J, Bang J, Kim J, Jin HJ, Kwak HW. Highly efficient Cr(VI) remediation by cationic functionalized nanocellulose beads. J Hazard Mater. 2022;426:128078. doi:10.1016/j.jhazmat.2021.128078.
89. Zhang W, Han X, You J, Zhang X, Pei D, Willför S, et al. Rapid and manual-shaking exfoliation of amidoximated cellulose nanofibrils for a large-capacity filtration capture of uranium. J Mater Chem A. 2022;10(14):7920–7. doi:10.1039/d1ta10357a.
90. Tewatia P, Kaushik V, Jyoti MS, Pathania D, Singhal S, Kaushik A. Highly fluorescent composite of boron nitride quantum dots decorated on cellulose nanofibers for detection and removal of Hg(II) ions from waste water. Int J Biol Macromol. 2023;234:123728. doi:10.1016/j.ijbiomac.2023.123728.

91. Silva NHCS, Figueira P, Fabre E, Pinto RJB, Pereira ME, Silvestre AJD, et al. Dual nanofibrillar-based bio-sorbent films composed of nanocellulose and lysozyme nanofibrils for mercury removal from spring waters. Carbohydr Polym. 2020;238:116210. doi:10.1016/j.carbpol.2020.116210.
92. Gomez-Maldonado D, Reynolds AM, Johansson LS, Burnett DJ, Ramapuram JB, Waters MN, et al. Fabrication of aerogels from cellulose nanofibril grafted with β-cyclodextrin for capture of water pollutants. J Porous Mater. 2021;28(6):1725–36. doi:10.1007/s10934-021-01109-w.
93. Tian C, She J, Wu Y, Luo S, Wu Q, Qing Y. Reusable and cross-linked cellulose nanofibrils aerogel for the removal of heavy metal ions. Polym Compos. 2018;39(12):4442–51. doi:10.1002/pc.24536.
94. Mo L, Shen Y, Tan Y, Zhang S. Ultralight and shapeable nanocellulose/metal-organic framework aerogel with hierarchical cellular architecture for highly efficient adsorption of Cu(II) ions. Int J Biol Macromol. 2021;193(Pt B):1488–98. doi:10.1016/j.ijbiomac.2021.10.212.
95. Nan Y, Gomez-Maldonado D, Iglesias MC, Whitehead DC, Peresin MS. Valorized soybean hulls as TEMPO-oxidized cellulose nanofibril and polyethylenimine composite hydrogels and their potential removal of water pollutants. Cellulose. 2023;30(6):3639–51. doi:10.1007/s10570-023-05086-y.
96. Chai F, Zhang R, Min X, Yang Z, Chai L, Zhao F. Highly efficient removal of arsenic (III/V) from groundwater using nZVI functionalized cellulose nanocrystals fabricated via a bioinspired strategy. Sci Total Environ. 2022;842:156937. doi:10.1016/j.scitotenv.2022.156937.
97. Banza M, Rutto H. Continuous fixed-bed column study and adsorption modeling removal of Ni^{2+}, Cu^{2+}, Zn^{2+} and Cd^{2+} ions from synthetic acid mine drainage by nanocomposite cellulose hydrogel. J Environ Sci Health Part A. 2022;57(2):117–29. doi:10.1080/10934529.2022.2036552.
98. Song M, Hu X, Gu T, Zhang WX, Deng Z. Nanocelluloses affixed nanoscale Zero-Valent Iron (nZVI) for nickel removal: synthesis, characterization and mechanisms. J Environ Chem Eng. 2022;10(3):107466. doi:10.1016/j.jece.2022.107466.
99. Hou X, Zhou H, Zhang J, Cai Y, Huang F, Wei Q. High adsorption pearl-necklace-like composite membrane based on metal-organic framework for heavy metal ion removal. Part Part Syst Charact. 2018;35(6):1700438. doi:10.1002/ppsc.201700438.
100. Chandra L, Vinothkumar K, Balakrishna RG. MIL-100 (Fe) integrated fibrous polyvinyl alcohol graft on cellulose acetate towards the development of green membranes; Application in multi solute rejection. J Environ Chem Eng. 2023;11(3):109851. doi:10.1016/j.jece.2023.109851.
101. Hazarika P, Duarah R, Goswami R, Rajguru P, Baruah S, Goswami PK, et al. Electrospun nanofibrous adsorptive membranes for removal of heavy metals from wastewater via a flow-through adsorption/permeation process. Chem Eng J. 2025;519:164877. doi:10.1016/j.cej.2025.164877.
102. Bhattacharya A, Sadaf A, Dubey S, Singh RP, Khare SK. Production and characterization of *Komagataeibacter xylinus* SGP8 nanocellulose and its calcite based composite for removal of Cd ions. Environ Sci Pollut Res Int. 2021;28(34):46423–30. doi:10.1007/s11356-020-08845-7.
103. Su K, Zhao D, Lu A, Zhong C, Shen XC, Ruan C. One-pot green synthesis of poly(hexamethylenediamine-tannic acid)-bacterial cellulose composite for the reduction, immobilization, and recovery of Cr(VI). J Environ Chem Eng. 2022;10(1):107026. doi:10.1016/j.jece.2021.107026.
104. Islam MM, Aidid AR, Mohshin JN, Mondal H, Ganguli S, Chakraborty AK. A critical review on textile dye-containing wastewater: ecotoxicity, health risks, and remediation strategies for environmental safety. Clean Chem Eng. 2025;11:100165. doi:10.1016/j.clce.2025.100165.
105. El-Sayed NS, Salama A, Guarino V. Coupling of 3-aminopropyl sulfonic acid to cellulose nanofibers for efficient removal of cationic dyes. Materials. 2022;15(19):6964. doi:10.3390/ma15196964.
106. Mahardiani L, Septianing P, Lesana P, Saputro S, Pranolo S. Nanofiber fabrication from palm fiber waste for sustainable water remediation. Moroc J Chem. 2022;10(2):337–50.
107. Tran-Ly AN, De France KJ, Rupper P, Schwarze FWMR, Reyes C, Nyström G, et al. Melanized-cationic cellulose nanofiber foams for bioinspired removal of cationic dyes. Biomacromolecules. 2021;22(11):4681–90. doi:10.1021/acs.biomac.1c00942.

108. Zhu W, Kim D, Han M, Jang J, Choi H, Kwon G, et al. Fibrous cellulose nanoarchitectonics on N-doped Carbon-based metal-free catalytic nanofilter for highly efficient advanced oxidation process. Chem Eng J. 2023;460:141593. doi:10.1016/j.cej.2023.141593.
109. Gomez-Maldonado D, Ponce S, Peresin MS. The applicability of cellulose—Tara Gum composite hydrogels as dye capture adsorbents. Water Air Soil Pollut. 2022;233(8):340. doi:10.1007/s11270-022-05818-z.
110. Sanchez LM, Espinosa E, Mendoza Zélis P, Morcillo Martín R, de Haro Niza J, Rodríguez A. Cellulose nanofibers/PVA blend polymeric beads containing *in-situ* prepared magnetic nanorods as dye pollutants adsorbents. Int J Biol Macromol. 2022;209:1211–21. doi:10.1016/j.ijbiomac.2022.04.142.
111. Dadigala R, Bandi R, Alle M, Park CW, Han SY, Kwon GJ, et al. Effective fabrication of cellulose nanofibrils supported Pd nanoparticles as a novel nanozyme with peroxidase and oxidase-like activities for efficient dye degradation. J Hazard Mater. 2022;436:129165. doi:10.1016/j.jhazmat.2022.129165.
112. Zhang J, Zhang X, Tian Y, Zhong T, Liu F. Novel and wet-resilient cellulose nanofiber cryogels with tunable porosity and improved mechanical strength for methyl orange dyes removal. J Hazard Mater. 2021;416:125897. doi:10.1016/j.jhazmat.2021.125897.
113. Zhang W, Yang K, Han X, Cai H, Lu W, Yuan Y, et al. Metal-organic frameworks decorated pomelo peel cellulose nanofibers membranes for high performance dye rejection. Colloids Surf A Physicochem Eng Aspects. 2022;649:129393. doi:10.1016/j.colsurfa.2022.129393.
114. Riva L, Pastori N, Panozzo A, Antonelli M, Punta C. Nanostructured cellulose-based sorbent materials for water decontamination from organic dyes. Nanomaterials. 2020;10(8):1570. doi:10.3390/nano10081570.
115. Mokhtari A, Sabzi M, Azimi H. 3D porous bioadsorbents based on chitosan/alginate/cellulose nanofibers as efficient and recyclable adsorbents of anionic dye. Carbohydr Polym. 2021;265:118075. doi:10.1016/j.carbpol.2021.118075.
116. Kumar M, Tiwari A, Randhawa JK. Electrospun nanofibers of α-hematite/polyacrylonitrile/calcium carbonate/cellulose triacetate as a multifunctional platform in, wastewater treatment and remineralisation. Desalination. 2022;541:116030. doi:10.1016/j.desal.2022.116030.
117. Ali ASM, El-Aassar MR, Hashem FS, Moussa NA. Surface modified of cellulose acetate electrospun nanofibers by polyaniline/β-cyclodextrin composite for removal of cationic dye from aqueous medium. Fibres Polym. 2019;20(10):2057–69. doi:10.1007/s12221-019-9162-y.
118. Mo J, Hu D, Liu X, Sun Y, Li X, Wang C, et al. Eco-friendly ZIF-67/rice straw-derived cellulose acetate electrospun nanofiber mats for efficient CO_2 capturing and selectivity removal of methyl orange dye. J Environ Chem Eng. 2022;10(6):108989. doi:10.1016/j.jece.2022.108989.
119. Elmaghraby NA, Omer AM, Kenawy ER, Gaber M, Hassaan MA, Ragab S, et al. Electrospun cellulose acetate/activated carbon composite modified by EDTA (rC/AC-EDTA) for efficient methylene blue dye removal. Sci Rep. 2023;13(1):9919. doi:10.1038/s41598-023-36994-5.
120. Dhar P, Kumar A, Katiyar V. Fabrication of cellulose nanocrystal supported stable Fe(0) nanoparticles: a sustainable catalyst for dye reduction, organic conversion and chemo-magnetic propulsion. Cellulose. 2015;22(6):3755–71. doi:10.1007/s10570-015-0759-z.
121. Shanmugarajah B, Chew IM, Mubarak NM, Choong TS, Yoo C, Tan K. Valorization of palm oil agro-waste into cellulose biosorbents for highly effective textile effluent remediation. J Clean Prod. 2019;210:697–709. doi:10.1016/j.jclepro.2018.10.342.
122. Zhao W, Chi H, Zhang S, Zhang X, Li T. One-pot synthesis of cellulose/MXene/PVA foam for efficient methylene blue removal. Molecules. 2022;27(13):4243. doi:10.3390/molecules27134243.
123. Thorat MN, Jagtap A, Dastager SG. Fabrication of bacterial nanocellulose/polyethyleneimine (PEI-BC) based cationic adsorbent for efficient removal of anionic dyes. J Polym Res. 2021;28(9):354. doi:10.1007/s10965-021-02702-y.
124. Vilela C, Moreirinha C, Almeida A, Silvestre AJD, Freire CSR. Zwitterionic nanocellulose-based membranes for organic dye removal. Materials. 2019;12(9):1404. doi:10.3390/ma12091404.

125. Bhuyan C, Konwar A, Bora P, Rajguru P, Hazarika S. Cellulose nanofiber-poly(ethylene terephthalate) nanocomposite membrane from waste materials for treatment of petroleum industry wastewater. J Hazard Mater. 2023;442:129955. doi:10.1016/j.jhazmat.2022.129955.
126. Huang W, Tao Y, Li Y, Luo T, Tang Y. Tannic acid-assisted construction of ZIF-8/cellulose nanofiber composite aerogels for efficient oil adsorption and oil/water separation. Carbohydr Polym. 2025;369:124283. doi:10.1016/j.carbpol.2025.124283.
127. Qu W, Wang Z, Qin M, Yang X, Zhang F, Wang Z, et al. Synthesis and characterization of UiO-66-NH_2 incorporated PVA/cellulose nanofibers composite aerogel for enhanced oil–water separation and formaldehyde adsorption. Sep Purif Technol. 2023;325:124673. doi:10.1016/j.seppur.2023.124673.
128. Li X, Yang Z, Peng Y, Zhang F, Lin M, Zhang J, et al. Self-powered aligned porous superhydrophobic sponge for selective and efficient absorption of highly viscous spilled oil. J Hazard Mater. 2022;435:129018. doi:10.1016/j.jhazmat.2022.129018.
129. Son D, Kim S, Kim J, Kim D, Ryu S, Lee Y, et al. Surface grafting of a zwitterionic copolymer onto a cellulose nanofiber membrane for oil/water separation. Cellulose. 2023;30(15):9635–45. doi:10.1007/s10570-023-05475-3.
130. Sultana N, Rahman R. Electrospun nanofiber composite membranes based on cellulose acetate/nano-zeolite for the removal of oil from oily wastewater. Emergent Mater. 2022;5(1):145–53. doi:10.1007/s42247-021-00326-y.
131. Wang D, Mhatre S, Chen J, Shi X, Yang H, Cheng W, et al. Composites based on electrospun fibers modified with cellulose nanocrystals and SiO_2 for selective oil/water separation. Carbohydr Polym. 2023;299:120119. doi:10.1016/j.carbpol.2022.120119.
132. Wu MB, Zhang C, Pi JK, Liu C, Yang J, Xu ZK. Cellulose nanocrystals as anti-oil nanomaterials for separating crude oil from aqueous emulsions and mixtures. J Mater Chem A. 2019;7(12):7033–41. doi:10.1039/c9ta00420c.
133. Wu J, Su Y, Cui Z, Yu Y, Qu J, Hu J, et al. Flexible, durable, and anti-fouling nanocellulose-based membrane functionalized by block copolymer with ultra-high flux and efficiency for oil-in-water emulsions separation. Nano Res. 2023;16(4):5665–75. doi:10.1007/s12274-022-5149-x.
134. Komal, Gupta K, Nidhi, Kaushik A, Singhal S. Amelioration of adsorptive efficacy by synergistic assemblage of functionalized graphene oxide with esterified cellulose nanofibers for mitigation of pharmaceutical waste. J Hazard Mater. 2022;424(Pt B):127541. doi:10.1016/j.jhazmat.2021.127541.
135. Jin Y, Ni Y, Pudukudy M, Zhang H, Wang H, Jia Q, et al. Synthesis of nanocrystalline cellulose/hydroxyapatite nanocomposites for the efficient removal of chlortetracycline hydrochloride in aqueous medium. Mater Chem Phys. 2022;275:125135. doi:10.1016/j.matchemphys.2021.125135.
136. Zhang H, Zheng Y, Zhou H, Zhu S, Yang J. Nanocellulose-intercalated MXene NF membrane with enhanced swelling resistance for highly efficient antibiotics separation. Sep Purif Technol. 2023;305:122425. doi:10.1016/j.seppur.2022.122425.
137. Liu J, Liu D, Liu S, Li Z, Wei X, Lin S, et al. Preparation and characterization of sulfated cellulose nanocrystalline and its composite membrane for removal of tetracycline hydrochloride in water. Energy Environ Mater. 2020;3(2):209–15. doi:10.1002/eem2.12055.
138. Jackson J, Moallemi A, Mu C, Plackett D. The use of surface-modified nanocrystalline cellulose integrated membranes to remove drugs from waste water and as polymers to clean oil sands tailings ponds. Polymers. 2021;13(22):3899. doi:10.3390/polym13223899.
139. Herrera-Morales J, Turley TA, Betancourt-Ponce M, Nicolau E. Nanocellulose-block copolymer films for the removal of emerging organic contaminants from aqueous solutions. Materials. 2019;12(2):230. doi:10.3390/ma12020230.
140. Mantripragada S, Dong M, Zhang L. Sustainable filter/adsorbent materials from cellulose-based electrospun nanofibrous membranes with soy protein coating for high-efficiency GenX fluorocarbon remediation from water. Cellulose. 2023;30(11):7063–78. doi:10.1007/s10570-023-05304-7.
141. Sorriaux M, Sorieul M, Chen Y. Bio-based and robust polydopamine coated nanocellulose/amyloid composite aerogel for fast and wide-spectrum water purification. Polymers. 2021;13(19):3442. doi:10.3390/polym13193442.

142. Lorevice MV, Claro PIC, Aleixo NA, Martins LS, Maia MT, Oliveira APS, et al. Designing 3D fractal morphology of eco-friendly nanocellulose-based composite aerogels for water remediation. Chem Eng J. 2023;462:142166. doi:10.1016/j.cej.2023.142166.
143. Lorevice MV, Mendonça EO, Orra NM, Borges AC, Gouveia RF. Porous cellulose nanofibril–natural rubber latex composite foams for oil and organic solvent absorption. ACS Appl Nano Mater. 2020;3(11):10954–65. doi:10.1021/acsanm.0c02203.
144. Sarvalkar PD, Vhatkar RS, Sharma KKK. Cellulose nanofiber-reinforced γ-AlOOH aerogels for enhanced removal of environmental pollutants. Langmuir. 2025;41(5):3475–89. doi:10.1021/acs.langmuir.4c04613.
145. Zhang F, Lian M, Alhadhrami A, Huang M, Li B, Mersal GAM, et al. Laccase immobilized on functionalized cellulose nanofiber/alginate composite hydrogel for efficient bisphenol A degradation from polluted water. Adv Compos Hybrid Mater. 2022;5(3):1852–64. doi:10.1007/s42114-022-00476-5.
146. Wang Z, Xia D, Cui S, Yu W, Wang B, Liu H. A high-capacity nanocellulose aerogel uniformly immobilized with a high loading of nano-$La(OH)_3$ for phosphate removal. Chem Eng J. 2022;433:134439. doi:10.1016/j.cej.2021.134439.
147. Kaur M, Kumar V, Sharma K, Saini S, Sharma M, Paulik C, et al. Tethering cellulose fibers with disulphide linkages for rapid and efficient adsorption of mercury ions and dye from wastewater: adsorption mechanism and process optimization using RSM. Sep Purif Technol. 2023;322:124275. doi:10.1016/j.seppur.2023.124275.
148. Lu W, Duan C, Zhang Y, Gao K, Dai L, Shen M, et al. Cellulose-based electrospun nanofiber membrane with core-sheath structure and robust photocatalytic activity for simultaneous and efficient oil emulsions separation, dye degradation and Cr(VI) reduction. Carbohydr Polym. 2021;258:117676. doi:10.1016/j.carbpol.2021.117676.
149. Hassan HMA, Alsohaimi IH, El-Aassar MR, El-Hashemy MA, El-Sayed MY, Alotaibi NF, et al. Electrospun TiO_2-GO/PAN-CA nanofiber mats: a novel material for remediation of organic contaminants and nitrophenol reduction. Environ Res. 2023;234:116587. doi:10.1016/j.envres.2023.116587.
150. Li W, Li T, Li G, An L, Li F, Zhang Z. Electrospun $H_4SiW_{12}O_{40}$/cellulose acetate composite nanofibrous membrane for photocatalytic degradation of tetracycline and methyl orange with different mechanism. Carbohydr Polym. 2017;168:153–62. doi:10.1016/j.carbpol.2017.03.079.
151. Peiravi-Rivash O, Mashreghi M, Baigenzhenov O, Hosseini-Bandegharaei A. Producing bacterial nano-cellulose and keratin from wastes to synthesize keratin/cellulose nanobiocomposite for removal of dyes and heavy metal ions from waters and wastewaters. Colloids Surf A Physicochem Eng Aspects. 2023;656:130355. doi:10.1016/j.colsurfa.2022.130355.
152. Sharma V, Shahnaz T, Subbiah S, Narayanasamy S. New insights into the remediation of water pollutants using nanobentonite incorporated nanocellulose chitosan based aerogel. J Polym Environ. 2020;28(7):2008–19. doi:10.1007/s10924-020-01740-9.
153. Luo X, Huang G, Chen X, Guo J, Yang W, Tang W, et al. Ingenious ambient temperature fabrication zirconium-metal organic framework laden polysaccharide aerogel as an efficient glyphosate scavenger. J Environ Chem Eng. 2021;9(6):106808. doi:10.1016/j.jece.2021.106808.
154. Wang Y, Guo Y, Yang C, Meng H, Li S, Sarp S, et al. Bio-inspired fabrication of adsorptive ultrafiltration membrane for water purification: simultaneous removal of natural organic matters, lead ion and organic dyes. J Environ Chem Eng. 2023;11(3):109798. doi:10.1016/j.jece.2023.109798.
155. Li C, Guo J, Xu P, Hu W, Lv J, Shi B, et al. Facile preparation of superior compressibility and hydrophobic reduced graphene oxide@cellulose nanocrystals/EPDM composites for highly efficient oil/organic solvent adsorption and enhanced electromagnetic interference shielding. Sep Purif Technol. 2023;307:122775. doi:10.1016/j.seppur.2022.122775.
156. Jiang J, Zhu J, Zhang Q, Zhan X, Chen F. A shape recovery zwitterionic bacterial cellulose aerogel with superior performances for water remediation. Langmuir. 2019;35(37):11959–67. doi:10.1021/acs.langmuir.8b04180.
157. Wahid F, Zhao XQ, Cui JX, Wang YY, Wang FP, Jia SR, et al. Fabrication of bacterial cellulose with TiO_2-ZnO nanocomposites as a multifunctional membrane for water remediation. J Colloid Interface Sci. 2022;620:1–13. doi:10.1016/j.jcis.2022.03.108.
158. Duan H, Wang M, Zhang Z, Zhen J, Lv W. Biomass-derived photothermal carbon aerogel for efficient solar-driven seawater desalination. J Environ Chem Eng. 2023;11(2):109295. doi:10.1016/j.jece.2023.109295.